

A Survey on RGB-D Datasets

Alexandre Lopes^a, Roberto Souza^b, Helio Pedrini^a

^a*Institute of Computing, University of Campinas, Brazil*

^b*Department of Electrical and Software Engineering, University of Calgary, Canada*

Abstract

RGB-D data is essential for solving many problems in computer vision. Hundreds of public RGB-D datasets containing various scenes, such as indoor, outdoor, aerial, driving, and medical, have been proposed. These datasets are useful for different applications and are fundamental for addressing classic computer vision tasks, such as monocular depth estimation. This paper reviewed and categorized image datasets that include depth information. We gathered 203 datasets that contain accessible data and grouped them into three categories: scene/objects, body, and medical. We also provided an overview of the different types of sensors, depth applications, and we examined trends and future directions of the usage and creation of datasets containing depth data, and how they can be applied to investigate the development of generalizable machine learning models in the monocular depth estimation field.

Keywords: RGB-D data, Monocular Depth Estimation, Computer Vision, Depth Datasets

1. Introduction

Depth is a critical information for many computer vision and image analysis applications. For example, it has been applied for tasks such as synthetic object insertion in computer graphics [1], robotic grasping [2] automatic 2D to 3D conversion in film [3], robot-assisted surgery [4], and autonomous driving [5].

Despite using depth sensors that capture the distance information, researchers also use stereo vision matching to infer it, especially for its condensed size and cost. Lately, deep learning methods are being used to produce more precise and dense depth maps. For example, they can improve finer-grained details [6], produce dense maps from sparse inputs [7], and refine depth for mirror surfaces [8].

An important field of study for depth is monocular depth estimation, especially because it does not require using depth sensors, reducing the size and cost of computer vision systems' setups. Also, it can be applied to existing monocular systems, that comprise the majority of image capturing systems available. For instance, Light Detection And Ranging (LIDAR) scanners usually cost thousands of dollars, and their cost and weight can be impractical for many small drone applications.

As a result of the extensive range of applications of depth, a considerable number of datasets include distance measurements of points of the scene they acquire. These datasets are collected using different sensors in distinct scenes for applications such as Simultaneous Localization and Mapping (SLAM) [9], Reconstruction [10], Object Segmentation [11], and Human Activity Recognition [12]. With the increasing number and diversity of datasets, researchers were able to explore more generalistic forms of depth estimation, leading to techniques focused on zero-shot cross-dataset depth estimation [13; 14; 15; 16]. The idea is to produce powerful methods able to estimate depth for in-the-wild scenes, increasing the range of applications for depth estimation.

The main contribution of this paper is to categorize and summarize the existing datasets with depth data. We propose a survey that can be used by researchers of both individual applications and general systems. While there are good reviews of RGB-D datasets [17; 18], the most recent one was published in 2017, and datasets have evolved both in complexity and size since then. Our survey presents a comprehensive literature review on more than 200 publicly available datasets included from an initial list of more than 300 datasets. Nearly half of the public datasets were published in 2017 or after, therefore, not included in any other review. We also made this work available on a website¹ to facilitate the filtering by application, scene type, sensor, and year.

The remainder of this paper is structured as follows. In the next section, we discuss and categorize depth sensors, explaining the main differences and applications for each category. In Section 3, we present the methodology used to perform the literature review. In Section 4, we present the datasets divided into categories, describing the most influential datasets for each category and presenting the rest in tables. In Section 5, we present tendencies and discuss future directions for RGB-D data usage. Finally, we provide a summary of the field and discuss how the area is evolving in Section 6.

2. Sensors

Range (or depth) data is crucial for understanding the 3D scene projected onto a 2D plane forming an image. There are multiple ways to obtain such information, either using a depth sensor or estimating depth. A depth sensor is a device that provides the distance from the sensor to an element in the scene, although it is possible to collect distance information using two or more RGB cameras from a scene. We define as Stereo Camera Sensing, all systems formed by two or more cameras. Therefore, light field cameras are also included here.

Previously, authors proposed distinct divisions for the types of sensors [19; 20]. In this survey, we use a categorization of depth sensors inspired by Choi [20]’s work. We divide the sensors into the following categories: Structured Light, Time-of-Flight (TOF), Light Detection and Ranging (LIDAR), and Stereo Camera Sensing. We display examples of each category in Figure 1.

Ultrasonic and Radar sensors also produce distance information, but they are out of the scope of this work because they are rarely used to produce depth information associated with RGB data. We detail each one of the sensors categories in the following sub-sections and show the differences of these types and possible application scenes in Table 1.

Table 1: Sensors overview comparing the usual application, distances and sparsity for each type of sensor.

Type	Typical Application Scenes	Typical Distance Usage	Sparsity
Structured Light	Indoor	Close Distances (0-10m)	Dense Map
TOF	Indoor	Close Distances (0-10m)	Dense Map
LIDAR	Aerial, Street, Outdoor, Indoor	Medium/Large Distances (10-1000m)	Sparse Map
Stereo Camera Sensing	Street, Outdoor, Indoor	Close/Medium Distances (0-100m)	Dense Map

2.1. Structured Light

Structured Light sensors (also called Active Stereo sensors) rely on a projector of light captured by a camera. The simplest way to achieve such a goal is to project a point with a device and capture this point in the scene with the camera. The depth of this point can be measured by a technique

¹www.alexandre-lobes.com/rgbd-datasets

called Triangulation. For estimating depth, it is necessary to find the position of the projected point in the image plane, have the distance between the camera and the light projector, the camera internal parameters, and the position in space of the projector. With this information, it is possible to create a triangle and calculate the height of the triangle formed by the camera, projector and illuminated scene point to determine the distance. The strategy of projecting points would be slow in practice since it is necessary to project a point for every position that is represented as a pixel in the image.

A more efficient strategy is to project the light as a stripe that associated with different coding strategies, such as the Binary Coded Structured Light strategy, can reduce the number of frames necessary to produce a full depth map. It can also be coded with RGB lights. Details about different codification strategies are discussed in [21].

Most Structured Light sensors do not work under direct sunlight since they rely on light projection in a scene. Therefore, they are usually suitable for indoor scene applications. Researchers have proposed strategies to overcome challenging light conditions [22], and now these sensors appear in smartphones for face identification systems for both indoor and outdoor scenes. They typically have a low range limit, not going further than 10 meters. Examples of this type of sensor include Matterport, Kinect v1, and RealSense SR300 cameras.

2.2. Time-of-Flight

TOF sensors rely on the time that a light wave takes to go to a point in a scene and to be reflected to a sensor. The concept is barely the same as the Ultrasonic and Radar Sensors, but here light is used as the emitted signal. The LIDAR sensors also work with the same approach, but they rely on one or multiple laser beams (concentrated light) to produce depth measurements of points in the scene, and the device usually has a rotating mirror to produce 360° scans of a scene. Hence, LIDAR sensors produce point clouds of a scene, not a dense depth map of it.

There are multiple strategies for capturing the time-of-flight of light. The most straightforward strategy is using Pulse Modulation, where a very fast pulse of light is emitted and then received by the sensor. Continuous Modulation is another strategy, where the light is modulated by its intensity, and the distance is measured by calculating the shift in phase of the original emitted light and the received light.

TOF sensors generally are compromised under strong sunlight conditions [23], making this sensor more commonly applied to indoor scenes. Existing studies try to overcome the effect under intense background light [24] and to reduce the measurement uncertainty under such conditions. Examples of this type of sensor include Kinect v2 (Xbox One sensor), SoftKinetic DS 325, and RIEGL VZ-400.

2.3. LIDAR

LIDAR sensors use the same idea of measuring the time that an emitted light is received by a sensor, but they rely on focused laser beams, which allow them to collect distance measurements as far as a few kilometers. LIDAR sensor models have different specifications (e.g., resolution, scans per second, and distance accuracy), and some scans are built in a multilayer (multiple laser beams) configuration, allowing them to measure not only in a 360° plane of the sensor but in 3D.

LIDAR measurement accuracy is usually independent of distance, although some models can fail in adverse weather conditions, such as dense fogs and turbulent snow [25]. Each LIDAR point also includes the intensity measurements, which can be interpreted as a measurement of reflectivity of the point that the light hit. This value is suitable for many applications, such as vegetation cover understanding and tunnel damage detection [26], giving LIDAR additional information that other types of sensors do not produce.

LIDAR sensors emit light; therefore, they work in difficult lighting conditions, such as dark environments. They are suitable for indoor and outdoor application scenes, but the available models are usually limited to specific applications, such as aerial measurements, outdoor/driving applications, and small indoor spaces depth estimation. Examples of such types of sensors include Velodyne Sensors, Faro Focus 3D Laser, and SICK LMS-511.

2.4. Stereo Camera Sensing

We define here Stereo Camera Sensing (SCS) as any system formed by two or more image sensors or lenses used to produce a Depth Map of a scene. Hence, simplistic pairs of cameras and complex light field systems composed by multiple microlenses are both identified in the same category. A straightforward strategy to measure depth from two or more cameras is Triangulation. The Triangulation idea is the same as applied in Structured Light sensors, but using a camera instead of a projector. The idea is that finding the position of a pixel in the image plane of camera A projected from a point P in the space, and the position of a pixel projected by the same point P in camera B , it is possible to find the depth of that point in a scene with the intrinsic parameters of the camera. After finding both lines projected in both cameras from point P , it is only necessary to know the distance between the two cameras (baseline distance) and internal parameters of the cameras to know the depth of the point P .

A limitation of this strategy occurs when the point of interest has no texture. For instance, it is practically impossible to determine which point of a smooth painted wall observed in the image projected by camera A is equivalent to the image projected by camera B . Therefore, it is difficult to determine a point's depth with acceptable accuracy without the correspondence of the pixels in both image planes. Recently, Deep Learning based methods have tried to address this limitation, increasing the accuracy of the estimation [27]. Examples of such types of sensors include light field cameras and ZED cameras.

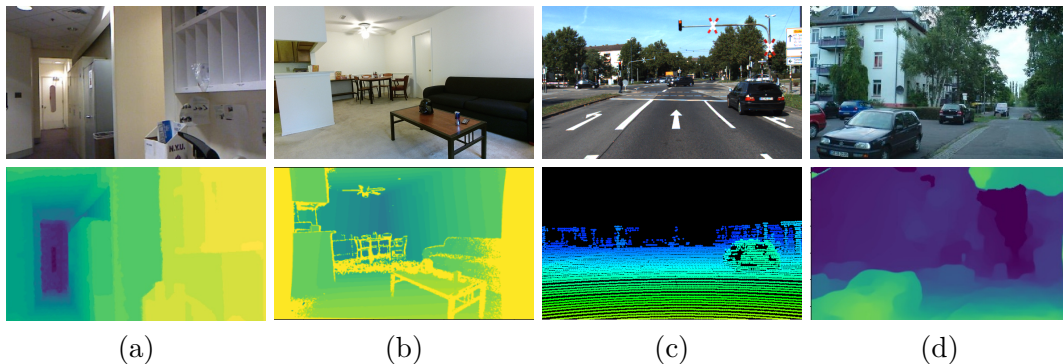


Figure 1: Examples of depth data with image (first row) and depth (second row) of the following sensors: **(a)** Structured Light from NYUv2 [28], **(b)** TOF from AVD [29], **(c)** LIDAR from KITTI [30], and **(d)** Stereo Camera Sensing from ReDWeb [31], where the authors compute correspondence maps by using optical flow.

3. Methodology

A literature review should synthesize previous knowledge, identify biases and gaps in the literature [32]. Since our study aims to describe, categorize, and identify future trends for RGB-D datasets, we defined a non-conventional methodology to find the related papers. Instead of defining search terms to find the papers directly, we collected datasets using backward snowballing.

The premise is that many datasets containing depth data do not have depth estimation as their primary goal, as in KITTI Dataset [30]. Therefore, defining search strings that could find depth datasets using generalist terms would result in numerous false-positive results. For instance, the search string `RGB-D OR Depth AND Dataset` searching in abstract, keywords, or title brings more than 23 thousand results in Scopus. Moreover, if we define a complex composed search string to filter the results, we would miss many datasets in the search.

As monocular depth estimation is a prominent field in the area, we defined the following search string to perform backward snowballing: `("single image" OR monocular) AND depth AND estimation`. The terms “monocular” and “single image” are applied mainly for monocular depth estimation but are also used for stereo trained systems, depth completion, and other applications. We conducted the review in Scopus and Google Scholar search engines. In Scopus, we revised all papers from January 1st, 2016, through August 31st, 2021. From Google Scholar, we followed the same dates, but we also included a stop criterion. If we found one search page without relevant items, we would end the year’s search. The inclusion of Google Scholar is justified because many relevant papers are published in Arxiv. Consequently, those could also be included in this work.

The exclusion and inclusion criteria for papers are defined in Table 2. These criteria are applied to the papers found using the previous search term. After excluding papers, backward snowballing was applied to find the datasets used/described by the remaining works. Initially, we reviewed 1,513 papers, which led to 305 dataset candidates. We also applied an exclusion criterion to these candidates, and only papers with active project websites, contact information to download the dataset, or direct download link were included. Hence, the final list of datasets to be included was reduced to 203 datasets.

Table 2: Inclusion and Exclusion Criteria.

Criterion	Category
Papers that discuss depth estimation	Inclusion
Papers using depth sensors, stereo image sensing, or synthetic data	Inclusion
Papers not written in English	Exclusion
Papers exclusively using private datasets	Exclusion
Papers not presenting minimal evidence of valid results	Exclusion
Duplicated paper/report. We kept the most complete one	Exclusion

4. Datasets

In recent years, many datasets have been created using the sensors or stereo vision sensing presented in the previous section. In addition to datasets using real data, this paper also includes datasets containing synthetic data. These were created mainly by simulation systems and often presented extra data such as semantic segmentation and 3D object detection bounding boxes. We divided the selected datasets into three different categories and six different sub-categories representing different application areas. The taxonomy tree is available in Figure 2.

The categories represent the intended application of the dataset. In the first level, we identify datasets that are mainly interested in Scenes/Objects, Human Body, or Medical Applications. The following sub-sections explore each application area, and list all of them in each sub-category’s table. We also detail three, two or one datasets for each sub-category, based on the total number of datasets of each sub-category. If we detail three papers, the two first ones are the most cited

papers that contain complementary scenarios. For example, KITTI Dataset and ScanNet Dataset contain street and indoor scenes, respectively. The third paper is the most cited paper published in 2017 or later. If we detail two papers, these are the most cited ones that contain complementary scenarios, and if we detailed one paper, it is the most cited in the sub-category.

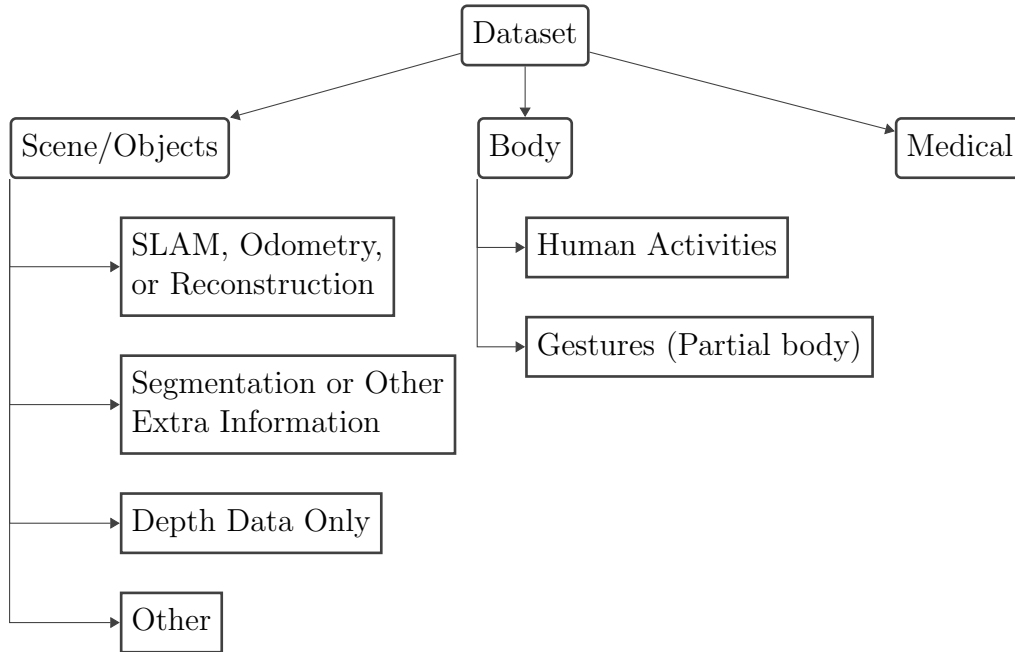


Figure 2: Taxonomy for RGB-D datasets.

4.1. Scene/Objects

In this category, we grouped all datasets intended to expose scenes, individual objects, or groups of objects. Therefore, datasets that reconstruct scenes/objects, segment elements of a scene, and contain exclusively depth maps are sub-categorized here. We created an “Other” sub-category to accommodate datasets that did not fit into these previous sub-categories.

Some papers explore multiple applications, primarily synthetic datasets, since they can create reconstruction and segmentation data directly using simulation environments. These papers are presented in one of their application areas to reduce redundancy. The only exception is for datasets of “SLAM, Odometry, or Reconstruction” and “Segmentation or Other Extra Information” sub-categories that are presented together in Table 5, since this combination is very frequent for datasets.

4.1.1. SLAM, Odometry, or Reconstruction

This sub-category contains multiple types of applications, however, all of them have a common characteristic: they present extra information that makes possible to recreate in any detail level, a 3D scene. For SLAM and odometry related papers, they typically present camera pose information, giving position and orientation of the capturing apparatus of each frame/image. We treated odometry differently from SLAM since odometry essentially aims to estimate the path of the camera, and SLAM tries to obtain a consistent trajectory and scene map of the camera [33].

All collected datasets that contain data exclusively for SLAM, Odometry, or Reconstruction are shown in Table 3. In general, applications of indoor scenes focus on reconstruction, and external scenes (such as driving scenes) focus on SLAM/odometry. Table 5 also contains datasets

of this sub-category, however, with extra annotated information such as semantic segmentation data. Some of the most cited datasets in the field include:

KITTI Dataset. Analyzing the datasets presented in this paper, this is the most cited one. The KITTI Dataset consists of a complex system of IMU/GPS, LIDAR scanner, and multiple cameras [30]. They recorded 6 hours of traffic scenes and, in addition to collecting the information from the sensors, provided data from 3D object detection bounding boxes, optical flow, and visual odometry/SLAM [86]. The project was expanded over the years, and the authors included data for tracking, road/lane detection, semantic/instance segmentation, and depth completion. Its depth completion data is composed of 94 thousand depth annotated RGB images [7] to produce dense depth maps from LIDAR points.

This dataset influenced the creation of the synthetic datasets Virtual KITTI [87] and Virtual KITTI 2 [88]. Recently, the KITTI authors released the KITTI-360 Dataset [89], which has more cameras, sensors, and more annotated data than the original KITTI Dataset.

ScanNet Dataset. ScanNet is an indoor dataset collected using an occipital structure sensor - a structured light sensor similar to Microsoft Kinect v1 [10]. The authors performed a dense reconstruction and conducted object instance-level annotation of all surfaces in the reconstruction. They also conducted a CAD Model Retrieval and Alignment for the objects in the scenes, which means that a 3D CAD model represented each instance of the annotated object in a scene. This dataset contains 2.5M views in 1,513 different scenes.

SunCG Dataset. The project associated with this dataset is focused on semantic scene completion, where from a single point of view, it estimates a complete 3D representation with the semantic label associated with the scene [90]. Instead of estimating the semantic segmentation of visible surfaces, this project aims to predict the occluded space (3D scene representation) and a label for each voxel in the scene. Therefore, it deals with Reconstruction and Segmentation as a unified task. This dataset comprises synthetic data containing an entire 3D model scene (which can be related to reconstruction), with semantic labels associated with it.

4.1.2. Segmentation or Other Extra Information

In this sub-category, all datasets have extra information that leads to a better scene understanding. Extra information can be seen as semantic or instance segmentation, 2D or 3D object detection, optical flow, etc. For instance, datasets that explore potential applications for depth estimation algorithms and semantic segmentation were categorized here.

Additionally, we provide the type of extra information of each dataset, and the complete list for every dataset is available in Table 4. Table 5 also reports datasets for this sub-category, as well as information of “SLAM, Odometry, or Reconstruction” sub-category. Therefore, researchers interested in semantic segmentation datasets may check both tables and refer to the “Extra Data” column to find the datasets that match their interest. Next, three of the most influencing and promising papers for this sub-category are presented.

NYUv2. This dataset contains indoor images and is the most cited dataset for this type of scene in the “Segmentation or Other Extra Information” sub-category. It was collected using Microsoft Kinect v1 sensor and is composed of aligned RGB and depth images, labeled data containing semantic segmentation, and raw data [28]. This project is a continuation of NYUv1[115], which uses the same sensor and type of data, but has fewer scenes and total frames.

Table 3: Datasets of “SLAM, Odometry, or Reconstruction” sub-category

Dataset Name	Ref.	Year	Scene Type	Sensor Type	Sensor Name	Data Modalities	Extra Data	Images/Scenes
GL3D	[34]	2018	Aerial	SCS	Stereo Camera	Color, Depth	-	543 Scenes (125623 Images)
ApolloScape	[35]	2020	Driving	LIDAR	Velodyne HDL-64E S3	Color, Depth, GPS, Radar	-	155 Min With 93k Frames
KAIST	[36]	2019	Driving	SCS, LIDAR	Velodyne VLP-16, SICK LMS-511, Stereo Camera	Color, Depth, GPS, IMU, Altimeter	-	19 Sequences (191 Km)
RobotCar	[37]	2016	Driving	LIDAR	2 X SICK LMS-151 2D LIDAR, 1 X SICK LD-MRS 3D LIDAR	Color, Depth, GPS, INS (Inertial Navigation System)	-	133 Scenes (almost 20M Images (from Multiple Sensors))
Malaga Urban	[38]	2014	Driving	SCS, LIDAR	2 SICK LMS, 3 HOKUYO, Stereo Camera	Color, Depth, IMU, GPS	-	15 Sequences
Omnidirectional	[39]	2014	Driving	SCS, LIDAR	Velodyne HDL-64E, Stereo Camera	Color, Depth	-	152 Scenes (12607 Frames)
Ford Campus Vision And Lidar	[40]	2011	Driving	SCS, LIDAR	Velodyne HDL-64E, Stereo Camera	Color, Depth, IMU, GPS	-	2 Sequences
Karlsruhe	[41]	2011	Driving	SCS	Stereo Camera	Color, GPS/IMU	-	20 Sequences (16657 Frames)
Multi-FoV (Urban Canyon)	[42]	2016	Driving, Indoor	-	Synthetic	Color, Depth	-	2 Sequences
-	[43]	2013	Driving, Outdoor	N/A	RGB-D Scans (N/A)	Color, Depth	-	13 Scenes (5 Castle, 5 Church, 3 Street Scenes)
BlendedStereo Camera	[44]	2020	In-the-wild	-	Synthetic	Color, Depth	-	113 Scenes (17k Images)
Youtube3D	[45]	2019	In-the-wild	-	Two Points Automatically Annotated	Color, Relative Depth	-	795066 Images
-	[46]	2019	In-the-wild	Structured Light, TOF	Kinect V1, V2 And Synthetic	Color, Depth	-	10 Scenes (2703 Frames)
4D Light Field Benchmark	[47]	2016	In-the-wild	-	Light-field (Synthetic)	Color, Depth	-	24 Scenes
Habitat Matterport (HM3D)	[48]	2021	Indoor	Structured Light	Matterport Pro2	Color, Depth	-	1000 Scenes
MilliEgo	[49]	2020	Indoor	Structured Light, LIDAR	Intel D435i Depth, Velodyne HDL-32E / Velodyne Ultra Puck	Radar, IMU, LIDAR, Depth	-	17 Distinct Floors From 6 Different Multistorey
ODS	[50]	2019	Indoor	SCS	MiniPolar 360 Camera (Stereo Camera)	Color, Depth	Normal Maps	6 Indoor Areas (50k Images)
360D	[51]	2018	Indoor	Structured Light	Synthetic And Matterport Camera	Color, Depth	-	12072 Scanned Scenes And 10024 CG Scenes
PanoSUNCG	[52]	2018	Indoor	-	Synthetic	Color, Depth	-	103 Scenes (25k Images)
CoRBS	[53]	2016	Indoor	TOF	Kinect V2	Color, Depth	-	4 Scenes (9 Hours Of Recording)
EuRoC MAV	[54]	2016	Indoor	TOF, Stereo Camera	Vicon Motion Capture, Leica MS50	Color, Depth, IMU	-	11 Scenes
Augmented ICL-NUIM	[55]	2015	Indoor	-	Synthetic	Color, Depth	-	4 Scenes (2 Living Room, 2 Offices)
Ikea	[56]	2015	Indoor	Structured Light	Kinect V1 And PrimeSense	Color, Depth	-	7 Scenes
ViDRILo	[57]	2015	Indoor	Structured Light	Kinect V1	Color, Depth	Semantic Category of the Scene	5 Sequences (22454 Images)
ICL-NUIM	[58]	2014	Indoor	-	Synthetic	Color, Depth	-	8 Scenes (4 Living Room, 4 Office)
MobileRGBD	[59]	2014	Indoor	TOF	Kinect V2	Color, Depth	-	3 Scenes (9.5 Hours Of Recording)
RGBD Object V2	[60]	2014	Indoor	Structured Light	Kinect V1	Color, Depth	-	14 Sequences
-	[61]	2014	Indoor	LIDAR	Faro Focus 3D Laser	Depth	-	40 Scenes (rooms From Three Offices)
RGB-D 7-Scenes	[62]	2013	Indoor	Structured Light	Kinect V1	Color, Depth	-	7 Scenes (500-1000 Frames/scene)
Reading Room	[63]	2013	Indoor	Structured Light	Asus Xtion Pro Live	Color, Depth	-	1 Scene
TUM-RGBD	[9]	2012	Indoor	Structured Light	Kinect V1	Color, Depth, Accelerometer	-	39 Sequences
IROS 2011 Paper Kinect	[64]	2011	Indoor	Structured Light	Kinect V1	Depth	-	27 Sequences
-	[65]	2013	Indoor, Isolated Objects / Focussed On Objects	Structured Light	Asus Xtion Pro Live	Color, Depth	-	6 Scenes
-	[66]	2012	Indoor, Isolated Objects / Focussed On Objects	Structured Light, TOF	KinectFusion (Kinect V1) For Two Scenes, Riegl VZ-400 For Office	Color, Depth	-	2 Scenes: Statue And Targetbox

Continue on Next Page

Dataset Name	Ref.	Year	Scene Type	Sensor Type	Sensor Name	Data Modalities	Extra Data	Images/Scenes
M&M	[67]	2020	Indoor, Outdoor	SCS	Stereo Camera	Color, Depth	-	4690 Sequences (170k Frames) And 130k Images
Mannequin Challenge	[68]	2019	Indoor, Outdoor	SCS	Stereo Camera	Color, Depth	-	4690 Sequences (170k Frames)
Stereo CameraEC	[69]	2018	Indoor, Outdoor	SCS, LIDAR	Velodyne (LIDAR), Stereo Camera	Color, Depth, IMU	-	5 Sequences
ETH3D	[70]	2017	Indoor, Outdoor	SCS, LIDAR	FaroFocus X 330 (Laser Sensor), Stereo Camera	Color, Depth	-	25 High-res, 10 Low-res
DiLigGent-MV	[71]	2020	Isolated Objects / Focussed On Objects	SCS	Stereo Camera	Color	-	5 Objects (scenes)
A Large Dataset of Object Scans	[72]	2016	Isolated Objects / Focussed On Objects	Structured Light	PrimeSense Carmine	Color, Depth	-	Over 10k 3D Scans Of Objects.
-	[73]	2015	Isolated Objects / Focussed On Objects	SCS, Structured Light	PrimeSense, Stereo Camera	Color, Depth	-	9 Scenes: 4 Scenes Using PrimeSense, 5 Scenes Using Stereo Camera
BigBIRD	[74]	2014	Isolated Objects / Focussed On Objects	Structured Light	Carmine 1.09 Sensor	Color, Depth	-	600 Images (from 125 Objects)
Fountain	[75]	2014	Isolated Objects / Focussed On Objects	Structured Light	Asus Xtion Pro Live	Color, Depth	-	1 Scene
MVS	[76]	2014	Isolated Objects / Focussed On Objects	SCS	Stereo Camera	Color	-	124 Scenes
The Newer College	[77]	2020	Outdoor	Structured Light, LIDAR	Intel D435i, Ouster OS-1 (Gen 1) 64	Color, Depth, IMU	-	6 Scenes
Megadepth	[78]	2018	Outdoor	SCS	Stereo Camera	Color, Depth	-	130k Images
CVC-13: Multimodal Stereo	[79]	2013	Outdoor	SCS	Stereo Camera	Color, Infrared	-	4 Scenes
Live Color+3D Database	[80]	2011	Outdoor	TOF	Range Scanner (RIEGL VZ-400)	Color, Depth	-	12 Scenes
Make3D	[81]	2009	Outdoor	TOF	Custom-built 3-D Scanner	Color, Depth	-	534 Images
Fountain-P11 And Herz-Jesu-P8	[82]	2008	Outdoor	LIDAR	N/A	Color, Depth	-	2 Scenes (19 Images)
-	[83]	2011	Partial Body W/o Scene	SCS	Stereo Camera (seven Cameras)	Color	-	N/A (2 Actors)
-	[84]	2016	Underwater	SCS	Stereo Camera	Color, Depth, IMU, Sonar	-	3 Sequences
DeMon	[85]	2017	N/A	SCS, Synthetic, Structured Light	Synthetic, Stereo Camera, Asus Xtion Pro Live, Kinect V1	Color, Depth	-	20537 Sequences And Scenes
Scenes11	[85]	2017	N/A	-	Synthetic	Color, Depth	-	19959 Sequences

Scene Flow Datasets. This dataset is a collection of three datasets: FlyingThing3D, Monkaa, and Driving. The first is composed of everyday objects flying along random trajectories [105]. The second was created using Blender computer graphics software, based on the information from an animated short film called Monkaa. The third is composed of a street scene. Scene Flow contains only synthetic data for all three datasets and, in addition to depth and RGB frames, the authors also include optical flow, segmentation, and stereo disparity change data.

Waymo Perception. This dataset is a street scene dataset composed of RGB and LIDAR labels. It consists of street scenes, and the authors labeled LIDAR using 3D bounding boxes for vehicles, pedestrians, cyclists, and signs [96]. They also provide RGB images annotations with 2D bounding boxes of vehicles, pedestrians, and cyclists. The 3D bounding boxes also have unique tracking IDs for tracking applications. The Waymo Perception Dataset is composed of 1,150 scenes with 20 seconds of recording each.

4.1.3. Depth Data Only

The datasets presented here are for the specific purpose of training depth estimation algorithms. They do not directly provide reconstruction, SLAM, or other information, although some of these applications are direct results of depth estimation. For example, these works explore monocular

Table 4: Datasets of “Segmentation” or “Other Extra Information”

Dataset Name	Ref.	Year	Scene Type	Application	Sensor Type	Sensor Name	Data Modalities	Extra Data	Images/Scenes
VALID	[91]	2020	Aerial	SOE	-	Synthetic	Color, Depth	Object Detection, Panoptic Segmentation, Instance Segmentation, Semantic Segmentation	6 Scenes (6690 Images)
US3D	[92]	2019	Aerial	SOE	LIDAR	Airborne LIDAR	Color, Depth	Semantic Segmentation	4160 Images From 3 Different Cities (a Fourth Is Not Available)
Vaihingen	[93]	2011	Aerial	SOE	LIDAR	Leica ALS50 And ALTM-ORION M	Color, Depth	Semantic Segmentation	33 Patches
Potsdam	[94]	2011	Aerial	SOE	N/A	N/A	Color, Depth	Semantic Segmentation	38 Patches
Leddar Pixset	[95]	2021	Driving	SOE and Tracking (Other)	LIDAR	Leddar Pixell LIDAR	Color, Depth, IMU, Radar	3D Bounding Boxes, 2D Bounding Boxes, Semantic Segmentation	97 Sequences (29k Frames)
Virtual Kitti 2	[88]	2020	Driving	SOE and Tracking (Other)	-	Synthetic	Color, Depth	Semantic Segmentation, Instance Segmentation, Optical Flow	5 Scenes (multiple Conditions For Each Scene)
Waymo Perception	[96]	2020	Driving	SOE	LIDAR	N/A	Color, Depth	3D Object Detection	1150 Scenes (20 Seconds/scene)
Argoverse	[97]	2019	Driving	SOE and Tracking (Other)	SCS, LIDAR	Argo LIDAR, Stereo Camera	Color, Depth	3D Object Detection	113 Scenes
CityScapes	[98]	2016	Driving	SOE	SCS	Stereo Camera	Color, Odometry	Semantic Segmentation, 3d-object Detection And Pose	50 Cities (25k Images)
SYNTHIA	[99]	2016	Driving	SOE	Virtual 8 Depth Sensors	Synthetic	Color, Depth	Instance Segmentation	5 Sequences (with Sub-sequences) At 5 Fps. 200k Images From Videos
Daimler Urban Segmentation	[100]	2014	Driving	SOE	SCS	Stereo Camera	Color	Semantic Labeling	5k Images
Ground Truth Stixel	[101]	2013	Driving	SOE	SCS	Stereo Camera	Color	Stixels	12 Sequences
Daimler Stereo Pedestrian	[102]	2011	Driving	SOE	SCS	Stereo Camera	Color	Object Detection	28919 Images
Unreal	[103]	2018	Driving, Outdoor	SOE	-	Synthetic	Color, Depth	Semantic Segmentation	21 Sequences (100k Images)
OASIS V2	[104]	2021	In-the-wild	SOE	-	From Human Annotation	Color, Depth	Normal Maps, Instance Segmentation	102k Images
OASIS	[104]	2020	In-the-wild	SOE	-	From Human Annotation	Color, Depth	Normal Maps, Instance Segmentation	140k Images
Scene Flow	[105]	2016	In-the-wild	SOE	-	Synthetic	Color	Optical Flow, Object Segmentation	2256 Scenes (39049 Frames)
RGBD Salient Object Detection	[106]	2014	In-the-wild	SOE	Structured Light	Kinect V1	Color, Depth	Saliency Maps	1000 Images
Saliency Detection On Light Field	[107]	2014	In-the-wild	SOE	SCS	Lytro Light Field (Stereo Camera)	Color, Depth	Saliency Maps	100 Images
MPI Sintel	[108]	2012	In-the-wild	SOE	-	Synthetic	Color, Depth	Optical Flow	35 Scenes (50 Frames/scene)
NYUv2-OC++	[109]	2020	Indoor	SOE	Structured Light	Kinect V1	Color, Depth, Accelerometer	Occlusion Boundaries Maps	1449 Images From NYUv2
Near-Collision Set	[110]	2019	Indoor	SOE	SCS, LIDAR	LIDAR (N/A), Stereo Camera	Color, Depth	2D Object Detection	13658 Sequences
SUN RGB-D	[111]	2015	Indoor	SOE	Structured Light And TOF	Intel RealSense 3D Camera, Asus Xtion LIVE PRO, Kinect V1 and V2	Color, Depth	Semantic Segmentation, Object Detection And Pose	10335 Images
TUW	[112]	2014	Indoor	SOE	Structured Light	ASUS Xtion ProLive RGB-D	Color, Depth	Object Instance Recognition	15 Sequences (163 Frames)
Willow And Challenge	[112]	2014	Indoor	SOE	Structured Light	Kinect V1	Color, Depth	Object Instance Recognition	24 Sequences (353 Frames) For Willow, 39 Sequences (176 Frames)
NYU Depth V2	[28]	2012	Indoor	SOE	Structured Light	Kinect V1	Color, Depth, Accelerometer	Semantic Segmentation	464 Scenes (407024 Frames) With 1449 Labeled Aligned RGB-D Images
-	[113]	2012	Indoor	SOE	Structured Light	Kinect V1	Color, Depth	Semantic Segmentation	3 Options. Large: 2 Sequences (397 Frames)

Continue on Next Page

Dataset Name	Ref.	Year	Scene Type	Application	Sensor Type	Sensor Name	Data Modalities	Extra Data	Images/Scenes
Berkeley B3DO	[114]	2011	Indoor	SOE	Structured Light	Kinect V1	Color, Depth	Object Detection	75 Scenes (849 Images)
NYU Depth V1	[115]	2011	Indoor	SOE	Structured Light	Kinect V1	Color, Depth	Semantic Segmentation	64 Scenes (108617 Frames) With 2347 Labeled RGB-D Frames
ClearGrasp	[116]	2019	Isolated Objects / Focussed On Objects	SOE	Structured Light	Synthetic, Intel RealSense D415	Color, Depth	Normal Maps, Semantic Segmentation - Synthetic	Over 50k Synthetic Images Of 9 Objects. 286 Real Images Of 10 Objects
T-LESS	[117]	2017	Isolated Objects / Focussed On Objects	SOE	Structured Light, TOF	Kinect V2, PrimeSense Carmine 1.0	Color, Depth	3D Instance Segmentation	N/A Scenes (38k Images) For Training. 20 Scenes (10k Images) For Testing
DROT	[118]	2016	Isolated Objects / Focussed On Objects	SOE	Structured Light, TOF	Kinect V1, V2 And RealSense R200	Color, Depth	Object Motion	5 Scenes (112 Frames)
MPII Multi-Kinect	[119]	2012	Isolated Objects / Focussed On Objects	SOE	SCS, Structured Light	Kinect V1, Stereo Camera	Color, Depth	Object Detection	33 Scenes (560 Images)
Mid-Air	[120]	2019	Outdoor	SOE	-	Synthetic	Color, Depth, Accelerometer, Gyroscope, GPS	Normal Maps, Semantic Segmentation	54 Sequences (420k Frames)

SOE: Segmentation or Other Extra Information

depth estimation [167], zero-shot depth estimation [149], and multi-camera depth estimation [145].

We present all papers found specifically for depth estimation in Table 6. All datasets for all categories and sub-categories in this paper also contain depth information as it is an inclusion criterion for papers to be incorporated to this work. Some relevant papers in this sub-category are:

ReDWeb Dataset. This dataset deals with the in-the-wild scenario, covering scenes such as street, office, park, farm, etc. As formed in the acronym of this dataset’s name “Relative Depth from Web” (ReDWeb), this dataset is formed by stereo images collected from the Internet [31]. The authors use optical flow to generate correspondence maps and create a relative depth map of the image. They post-process the data by segmenting the sky to increase the quality of the depth maps.

SQUID Dataset. This dataset is composed of underwater images collected from four different sites: two in the Red Sea and two in the Mediterranean Sea [166]. In addition to collecting stereo pair images, the authors included a ColorChecker to propose color restoration techniques in underwater images.

Middlebury Datasets. These datasets are a composition of data released in different papers over the years of 2001, 2003, 2005, 2006, and 2014. These datasets are acquired using different strategies: custom structured light using a video projector for the Middlebury 2003 [162], Middlebury 2005 [161; 168], Middlebury 2006 [161; 168], and Middlebury 2014 [160], while Middlebury 2001 [169] uses stereo image pair disparities. Despite using a custom structure light system, Middlebury 2014 contains improvements in the acquisition process.

4.1.4. Other

This sub-category contains all datasets that do not fit into the previous divisions. There is no sub-category in “Other” with more than four examples. Therefore, we did not create a specific sub-section for them.

All datasets here contain depth data and are divided into the following applications: novel view synthesis, foggy images for visibility restoration, relative depth between pairs of random points, object tracking, depth refinement for mirror surfaces, and synthesis of 4D RGB-D light

Table 5: Datasets of “SLAM, Odometry, or Reconstruction” and “Segmentation or Other Extra Information” Categories”

Dataset Name	Ref.	Year	Scene Type	Application	Sensor Type	Sensor Name	Data Modalities	Extra Data	Images/Scenes
-	[121]	2020	Aerial	SOR and SOE	-	Synthetic	Color, Depth	Normal Maps, Edges, Semantic Labels	15 Scenes (144k Images)
EventScape	[122]	2021	Driving	SOR and SOE	-	Synthetic	Color, Depth	Semantic Segmentation, Navigation Data (Position, Orientation, Angular Velocity, Etc)	758 Sequences
KITTI-360	[89]	2021	Driving	SOR and SOE	SCS, LIDAR	Velodyne (LIDAR) Points Cloud, Stereo Camera	Color, Depth, GPS, IMU	2d-object Detection, 3d-object Detection, Tracking, Instance Segmentation, Optical Flow. These Are Not In Necessary In The Same Dataset	11 Sequences To Over 320k Images And 100k Laser Scans
DDAD	[123]	2020	Driving	SOR and SOE	LIDAR	Luminar-H2 LIDAR	Color, Depth	Instance Segmentation	150 Scenes (12650 Frames)
Lyft Level 5	[124]	2020	Driving	SOR and SOE	SCS, LIDAR	3 LIDAR (40 And 64-beam Lidars), 5 Radars, Stereo Camera	Color, Depth, Radar	3d Object Detection	170k Scenes (25 Seconds Each)
NuScenes	[125]	2020	Driving	SOR and SOE	LIDAR	N/A	Color, Depth, Radar, IMU	3D Object Detection, Semantic Segmentation	1000 Scenes (20 Seconds Each). 1.4M Images And 390k Lidar Sweeps
Woodscape	[126]	2019	Driving	SOR and SOE	LIDAR	Velodyne HDL-64E	Color, IMU, GPS, Depth	Instance Segmentation, 2d Object Detection	50 Sequences (100k Frames)
Virtual Kitti	[87]	2016	Driving	SOR and SOE	-	Synthetic	Color, Depth	Semantic Segmentation, Instance Segmentation, Optical Flow	50 Videos (21260 Frames)
KITTI	[30]	2012	Driving	SOR and SOE	SCS, LIDAR	Velodyne (LIDAR) Points Cloud, Stereo Camera	Color, Grayscale, Depth, GPS, IMU	Instance Segmentation	61 Scenes (42746 Frames)
Hypersim	[127]	2021	Indoor	SOR and SOE	-	Synthetic	Color, Depth	Normal Maps, Instance Segmentation, Diffuse Reflectance	461 Scenes (77400 Images)
RoboTHOR	[128]	2020	Indoor	SOR and SOE	-	Synthetic	Color, Depth	Instance Segmentation	75 Scenes
Structured3D	[129]	2020	Indoor	SOR and SOE	-	Synthetic	Color, Depth	Object Detection, Semantic Segmentation	3500 Scenes With 21835 Rooms (196515 Frames)
Replica	[130]	2019	Indoor	SOR and SOE	Structured Light	N/A	Color, Depth, IMU, Grayscale Camera	Normal Maps, Instance Segmentation	18 Scenes
Gibson	[131]	2018	Indoor	SOR and SOE	LIDAR, Structured Light	NavVis, Matterport Camera, DotProduct	Color, Depth	Normal Maps, Semantic Segmentation	572 Scenes. 1400 Floor Spaces From 572 Buildings
InteriorNet	[132]	2018	Indoor	SOR and SOE	-	Synthetic	Color, Depth, IMU	Normal Maps, Semantic Segmentation	20 Million Images
Taskonomy	[133]	2018	Indoor	SOR and SOE	Structured Light	N/A	Color, Depth	25 Tags (Normals Maps, Semantic Segmentation, Scene Classification, Etc.)	4.5 Million Scenes
AVD	[29]	2017	Indoor	SOR and SOE	TOF	Kinect V2	Color, Depth	Object Detection	15 Scenes (over 30k Images)
MatterPort3D	[134]	2017	Indoor	SOR and SOE	SCS, Structured Light	Matterport Camera, Stereo Camera	Color, Depth	Semantic Segmentation, 3D Semantic-voxel Segmentation	90 Scenes, 10800 Panoramic Views (194400 Images)
ScanNet	[10]	2017	Indoor	SOR and SOE	Structured Light	Occipital Structure Sensor - Similar to Kinect V1	Color, Depth	3D Semantic-voxel Segmentation	1513 Sequences (over 2.5 Million Frames)
SceneNet RGB-D	[11]	2017	Indoor	SOR and SOE	-	Synthetic	Color, Depth	Instance Segmentation, Optical Flow	15K Trajectories (scenes) (5M Images)

Continue on Next Page

Dataset Name	Ref.	Year	Scene Type	Application	Sensor Type	Sensor Name	Data Modalities	Extra Data	Images/Scenes
SunCG	[90]	2017	Indoor	SOR and SOE	-	Synthetic	Color, Depth	Semantic Segmentation	45622 Scenes
GMU Kitchen	[135]	2016	Indoor	SOR and SOE	TOF	Kinect V2	Color, Depth	Object Detection	9 Scenes (6735 Frames)
Stanford2D3D	[136]	2016	Indoor	SOR and SOE	Structured Light	Matterport Camera	Color, Depth	Semantic Segmentation, Normal Maps	6 Large-scale Indoor Areas (70496 Images)
SUN3D	[137]	2013	Indoor	SOR and SOE	Structured Light	Asus Xtion Pro Live	Color, Depth	Semantic Segmentation	415 Sequences
Starter	[138]	2021	Indoor, In-the-wild	SOR And SOE (depending On Subdataset)	Structured Light	Synthetic, Matterport Pro2, NA	Color, Depth, IMU, Grayscale Camera (depending On Subdataset)	Semantic Segmentation, Normals Maps, Scene Classification, Etc. (depending On Subdataset)	Over 14.6M Images (multiple Scenes)
RGBD Object	[139]	2011	Indoor, Isolated Objects / Focussed On Objects	SOR and SOE	Structured Light	Kinect V1	Color, Depth	3d Segmentation	8 Sequences And 300 Isolated Objects (250k Frames)
TartanAir	[140]	2020	Indoor, Outdoor	SOR and SOE	-	Synthetic LIDAR	Color, Depth	Semantic Segmentation, Optical Flow	1037 Scenes (Over 1M Frames). Each Scene Contains 500-4000 Frames.
RGB-D Semantic Segmentation	[141]	2011	Isolated Objects / Focussed On Objects	SOR and SOE	Structured Light	Kinect V1	Color, Depth	3D Semantic Segmentation	16 Test Scenes
GTA-SfM	[142]	2020	Outdoor	SOR and SOE	-	Synthetic	Color, Depth	Optical Flow	76k Images

SOR: SLAM, Odometry, or Reconstruction
SOE: Segmentation or Other Extra Information

field images. In Table 7, we display all these datasets and their respective application as a column of the table. The most cited dataset included here is:

FRIDA2 This dataset is a synthetic dataset of foggy images of the street view. It is formed by 330 synthetic images of 66 different scenes, where each image without fog is associated with four images that vary the intensity of the artificial fog presented in it [170]. Therefore, 66 images without fog have one depth map and four foggy images associated with it. FRIDA2 is a continuation of The Foggy Road Image Database (FRIDA) [171], which has similar characteristics to FRIDA2, but fewer images (only 18 distinct scenes). These datasets are created for image enhancement in foggy images, trying to reduce the impact of the fog in the visibility of street scenes.

4.2. Body

In this category, all datasets are focused on body activities, such as action recognition, facial expression, hand activities, and sign language recognition. Here, we have only two sub-categories: the first one encompass full-body activities and the second one includes partial body parts, such as hands or face.

It is essential to notice that some of these datasets also include depth maps of the scene, but the focus of the dataset is on the Human Body (or part of it). Therefore, they are classified in this category.

4.2.1. Human Activities

This sub-category has all datasets focused on human activities, such as drinking, eating, playing tennis, and walking. Here, we have datasets that analyze actions for an individual person [178; 179] or two-person interactions [180].

The majority of the works in the “Human Activities” sub-category are collected in controlled scenes, and we only found Hollywood 3D [181] using in-the-wild datasets. The most common extra data is the person pose (or skeleton) of the people involved in the scene. Such information can help improve automatic action recognition algorithms. Datasets containing Human Activities

Table 6: Datasets of “Depth Data Only” sub-category

Dataset Name	Ref.	Year	Scene Type	Sensor Type	Sensor Name	Data Modalities	Extra Data	Images/Scenes
Espada	[143]	2021	Aerial	-	Synthetic	Color, Depth	-	49 Environments (80k Images)
DSEC	[144]	2021	Driving	SCS, LIDAR	Velodyne VLP-16, Stereo Camera	Color, Depth, GPS	-	53 Sequences
Mapillary	[145]	2020	Driving	SCS	Stereo Camera	Color, Depth	-	50k Scenes (750k Images)
RabbitAI Benchmark	[146]	2020	Driving	SCS	17-camera Light-field	Color	-	200 Scenes (100 For Training, 100 For Testing)
DrivingStereo - Driving Stereo	[147]	2019	Driving	SCS, LIDAR	Velodyne HDL-64E, Stereo Camera	Color, Depth, IMU, GPS	-	42 Sequences (182188 Frames)
Urban Virtual (UVD)	[148]	2017	Driving	-	Synthetic	Color, Depth	-	58500 Images
DiverseDepth	[149]	2020	In-the-wild	SCS	Stereo Camera	Color	-	320k Images
HRWSI	[150]	2020	In-the-wild	SCS	Stereo Camera	Color, Depth	-	20778 Images
Holopix50k	[151]	2020	In-the-wild	SCS	Stereo Camera	Color	-	49368 Images
DualPixels	[152]	2019	In-the-wild	SCS	Stereo Camera	Color, Depth	-	3190 Images
TAU Agent	[153]	2019	In-the-wild	-	Synthetic	Color, Depth	-	5 Scenes
WSVD	[154]	2019	In-the-wild	SCS	Stereo Camera	Color, Depth	-	553 Videos (1.5M Frames)
ReDWeb	[31]	2018	In-the-wild	SCS	Stereo Camera	Color, Depth	-	3600 Images
AirSim Building_99	[155]	2021	Indoor	-	Synthetic	Color, Depth	-	20k Images
Pano3D	[156]	2021	Indoor	LIDAR, Structured Light	3 RGB Cameras. The 3 Depth Cameras. Matterport Camera, NavVis, DotProduct (depending On Subdataset)	Color, Depth	Normal Maps	42923 Samples
Multiscopic Vision	[157]	2020	Indoor	-	Synthetic	Color	-	Around 1200 Scenes Of Synthetic Data, 92 Scenes Of Real Data.
IRS	[158]	2019	Indoor	-	Synthetic	Color, Depth	Normal Maps	100025 Images
IBims-1	[159]	2019	Indoor	TOF	Laser (Leica HDS7000 Laser Scanner)	Color, Depth	Semantic Segmentation (only For Planar Areas: Walls, Tables, Floor)	100 Images
Middlebury 2014	[160]	2014	Indoor	SCS	Stereo Camera	Color, Depth	-	33 Images
Middlebury 2006	[161]	2006	Indoor	Structured Light	Custom-build Structured Light	Color, Depth	-	21 Images
Middlebury 2005	[161]	2005	Indoor	Structured Light	Custom-build Structured Light	Color, Depth	-	9 Images
Middlebury 2003	[162]	2003	Indoor	Structured Light	Custom-build Structured Light	Color, Depth	-	2 Images
Middlebury 2001	[162]	2001	Indoor	SCS	Stereo Camera	Color, Depth	-	6 Images
DIODE	[163]	2019	Indoor, Outdoor	LIDAR	FARO Focus S350	Color, Depth	Normal Maps	30 Scenes (8574 Indoor Images, 16884 Outdoor Images)
DIML/CVL	[164]	2016, 2017, 2018, 2021	Indoor, Outdoor	SCS, TOF	Kinectv2 For Indoor, ZED Stereo Camera for Outdoor	Color, Depth	-	More Than 200 Scenes
Forest Virtual (FVD)	[148]	2017	Outdoor	-	Synthetic	Color, Depth	-	49500 Images
Zurich Forest	[148]	2017	Outdoor	SCS	Stereo Camera	Color, Depth	-	3 Sequences (9846 Images)
-	[165]	2021	Underwater	SCS	Stereo Camera	Color, Depth	-	600 Pairs (51 With Depth Ground Truth)
SQUID	[166]	2020	Underwater	SCS	Stereo Camera	Color, Depth	-	57 Images

are presented in Table 8. Next, we present two influential datasets in this sub-category:

MSR DailyActivity3D Dataset. This dataset covers sixteen different activities: drink, eat, read a book, call cellphone, write on a paper, use a laptop, use a vacuum cleaner, cheer up, sit still, toss paper, play games, lie down on a sofa, walk, play guitar, stand up, and sit down [178]. Ten subjects performed each action twice: one for standing and one for sitting position. This

Table 7: “Other” Scene/Objects RGB-D Datasets

Dataset Name	Ref.	Year	Scene Type	Application	Sensor Type	Sensor Name	Data Modalities	Extra Data	Images/Scenes
FRIDA2	[170]	2012	Driving	Fog (Other)	-	Synthetic	Color, Depth	-	66 Scenes (330 Images)
FRIDA	[171]	2010	Driving	Fog (Other)	-	Synthetic	Color, Depth	-	18 Scenes (90 Images)
3D Ken Burns	[172]	2019	In-the-wild	3D Ken Burns (Other)	-	Synthetic	Color, Depth	Normal Maps	46 Sequences
DIW	[173]	2016	In-the-wild	Points (Other)	-	Two Points (manually Annotated)	Color, Depth Points (2 Points)	-	495k Images
Mirror3D	[174]	2021	Indoor	Mirror (Other)	Structured Light, SCS	Matterport Camera, Stereo Camera, Kinect V1, Occipital Structure Sensor - Similar To Kinect V1	Color, Depth	Mirror Mask	7011 Scenes With Mirror
Princeton Tracking Benchmark	[175]	2013	Indoor	Tracking (Other)	Structured Light	Kinect V1	Color, Depth	-	100 Sequences
Dynamic Scene	[176]	2020	Indoor, Outdoor	Novel View Synthesis (Other)	SCS	Stereo Camera	Color	Semantic Segmentation	9 Scenes
LightField	[177]	2017	Other (Flowers)	Synthesizes A 4D RGBD LF (Other)	SCS	Lytro Illum (Light Field) (Stereo Camera)	Color	-	3343 Images

dataset also includes person pose information for each frame. The authors used the Kinect V1 to acquire the depth of the scenes.

MSR Action3D. This dataset covers twenty different actions performed by ten subjects. Each action was performed two to three times, resulting in 557 filtered sequences and 23797 frames [196]. The actions are divided into three sets, where the first categorize actions with similar movements. The third set is composed by complex actions together. All sequences were acquired using Kinect V1 sensor.

4.2.2. Gestures (Partial Body)

Here, we grouped all works that involve human actions or activities and have data available for human body parts, such as arms, head, and hand. There is a wide variety of dataset purposes in this sub-category, such as action recognition based on a first-person view (no torso/head parts available in video) [202], salad preparation [203], hand-pose information [204], and sign language recognition [205].

The most cited datasets in this sub-category include:

NYU Hand Pose Dataset. This dataset was captured using three Kinects v1, with two side views and a frontal view. The authors also re-created a synthetic hand pose for each view [204], and made available 36 hand point locations for each frame. Three people acquired the data: one person used for training and the other two for testing, leading to over 80 thousand acquired frames.

MSR Gesture3D. This dataset contains sign language gestures. The authors collected 12 dynamic American Sign Language (ASL) gestures from ten people. The dataset was captured using Kinect v1, and has 336 sequences since each person performed multiple recordings of all selected signs. The authors performed a hand segmentation, and depth information is available only for the segmented hand regions. Background and body portions below the wrist were removed.

4.3. Medical

In this category, we present datasets that are from any part of the medical field. The exclusion criteria removed most of the datasets found here because these contained only private data. For

Table 8: Datasets of “Human Activity” sub-category

Dataset Name	Ref.	Year	Scene Type	Sensor Type	Sensor Name	Data Modalities	Extra Data	Images/Scenes
-	[182]	2019	Full Body	TOF	Kinect V2	Color, Depth	-	800 Frames For Each Person (26 People)
UOW Online Action3D	[183]	2018	Full Body	TOF	Kinect V2	Color, Depth	Person Pose (Skeleton)	20 Sequences (20 Participants Performing Multiple Actions In A Sequence)
TVPR	[184]	2017	Full Body	Structured Light	Asus Xtion Pro Live	Color, Depth	-	23 Sequences (100 People, 2004 Secs)
TST Fall Detection V2	[185]	2016	Full Body	TOF	Kinect V2	Color, Depth, Accelerometer	Person Pose (Skeleton)	264 Scenes
UOW LargeScale Combined Action3D	[12]	2016	Full Body	TOF	Kinect V2	Color, Depth	Person Pose (Skeleton)	4953 Sequences
TST Intake Monitoring V1	[186]	2015	Full Body	Structured Light	Kinect V1	Color, Depth	-	48 Sequences
TST Intake Monitoring V2	[186]	2015	Full Body	Structured Light	Kinect V1	Color, Depth	-	60 Sequences
TST TUG DataBase	[187]	2015	Full Body	TOF	Kinect V2	Color, Depth, Accelerometer	Person Pose (Skeleton)	60 Sequences
UTD-MHAD	[188]	2015	Full Body	Structured Light	Kinect V1	Color, Depth, Accelerometer	Person Pose (Skeleton)	861 Sequences
Human3.6M	[189]	2014	Full Body	TOF	MESA Imaging SR4000 From SwissRanger	Color, Depth, Motion Capture (mx) Camera	Person Pose (Skeleton)	447260 RGB-D Frames (almost 3.6M RGB Frames)
Northwestern-UCLA Multiview Action 3D	[179]	2014	Full Body	Structured Light	Kinect V1	Color, Depth	-	1473 Sequences
TST Fall Detection V1	[190]	2014	Full Body	Structured Light	Kinect V1	Color, Depth, Accelerometer	Person Pose (Skeleton)	20 Sequences
Chalearn Multimodal Gesture Recognition	[191]	2013	Full Body	Structured Light	Kinect V1	Color, Depth, Audio	User Mask, Person Pose (Skeleton)	707 Sequences (1720800 Frames)
MHAD	[192]	2013	Full Body	Structured Light	Kinect V1	Color, Depth, Accelerometer, Motion Capture System	-	660 Sequences
ChaLearn Gesture Challenge	[193]	2012	Full Body	Structured Light	Kinect V1	Color, Depth	-	50k Sequences
DGait	[194]	2012	Full Body	Structured Light	Kinect V1	Color, Depth	-	583 Sequences (53 Subjects)
MSR DailyActivity3D	[178]	2012	Full Body	Structured Light	Kinect V1	Color, Depth	Person Pose (Skeleton)	320 Sequences
RGBD-ID	[195]	2012	Full Body	Structured Light	Kinect V1	Color, Depth	Person Pose (Skeleton)	316 Sequences (79 People)
SBU Kinect Interaction	[180]	2012	Full Body	Structured Light	Kinect V1	Color, Depth	Person Pose (Skeleton)	21 Sequences From Seven Participants
MSR Action3D	[196]	2010	Full Body	Structured Light	Similar to Kinect V1 (N/A)	Color, Depth	-	557 Sequences (23797 Frames)
Hollywood 3D	[181]	2013	In-the-wild	SCS	Stereo Camera	Color, Depth	-	Around 650 Video Clips
Depth 2 Height	[197]	2020	Indoor	TOF	Kinect V2	Color, Depth	-	2136 Images
HHOI	[198]	2016	Indoor	TOF	Kinect V2	Color, Depth	Person Pose (Skeleton)	8 Actors Recorded Interactions. Each Interaction Lasts 2-7 Seconds Presented At 10-15 Fps
CMU Panoptic	[199]	2015	Indoor	TOF	Kinect V2	Color, Depth	3D Skeleton	65 Sequences (5.5 Capture Hours)
UR Fall Detection	[200]	2014	Indoor	Structured Light	Kinect V1	Color, Depth, Accelerometer	-	70 Sequences
RGB-D People	[201]	2011	Indoor	Structured Light	Kinect V1	Color, Depth	Object Detection And Tracking	1 Sequence (1132 Frames Of 3 Sensors)

instance, we collected eleven datasets containing endoscopic data, but only three meets all criteria to be included in our work. This situation is common in medical applications as sharing medical information requires regulated procedures.

Table 9: Datasets of “Gestures (Partial Body) sub-category”

Dataset Name	Ref.	Year	Scene Type	Sensor Type	Sensor Name	Data Modalities	Extra Data	Images/Scenes
50 Salads	[203]	2013	Part Of Body (hand, Head, Etc.)	Structured Light	Kinect V1	Color, Depth, Accelerometer	Activity Classification	50 Sequences (25 People)
RGB2Hands	[206]	2020	Part Of Body (hand, Head, Etc.)	Structured Light	Intel RealSense SR300/Synthetic	Color, Depth	Segmentation, 2D Keypoints, Dense Matching Map, Inter-hand Distance, Intra-hand Distance	Real: 4 Sequences (1724 Frames). Synthetic: NA
ObMan	[207]	2019	Part Of Body (hand, Head, Etc.)	-	Synthetic	Color, Depth	3D Hand Keypoints, Object Segmentation, Hand Segmentation	150k Images
-	[133]	2018	Part Of Body (hand, Head, Etc.)	Structured Light	Intel RealSense SR300	Color, Depth, Magnetic And Kinematic Sensors	-	1175 Sequences (over 100k Frames)
BigHand2.2M	[208]	2017	Part Of Body (hand, Head, Etc.)	Structured Light	Intel RealSense SR300	Color, Depth, 6D Magnetic Sensor	-	N/A Sequences (2.2 Million Images), 10 Subjects
Pandora	[209]	2017	Part Of Body (hand, Head, Etc.)	TOF	Kinect V2	Color, Depth	Upper Body Part Person Pose (Skeleton)	100 Sequences (more Than 250k Frames) From 20 Subjects
RHD	[210]	2017	Part Of Body (hand, Head, Etc.)	-	Synthetic	Color, Depth	Segmentation, Keypoints	43986 Images
THU-READ	[202]	2017	Part Of Body (hand, Head, Etc.)	Structured Light	PrimeSense Carmine	Color, Depth	-	1920 Sequences
STB	[211]	2016	Part Of Body (hand, Head, Etc.)	SCS, Structured Light	Intel Real Sense F200, Stereo Camera	Color, Depth	-	12 Sequences (18k Images)
EYEDIAP	[212]	2014	Part Of Body (hand, Head, Etc.)	Structured Light	Kinect V1	Color, Depth	Eye Points, Head Pose	94 Sequences
Eurecom Kinect Face	[213]	2014	Part Of Body (hand, Head, Etc.)	Structured Light	Kinect V1	Color, Depth	Face Points	936 Sequences
MANIAC	[214]	2014	Part Of Body (hand, Head, Etc.)	Structured Light	Kinect V1	Color, Depth	-	103 Sequences
NYU Hand Pose	[204]	2014	Part Of Body (hand, Head, Etc.)	Structured Light	Synthetic/Kinect V1	Color, Depth	Hand Pose	81009 Frames
3DMAD	[215]	2013	Part Of Body (hand, Head, Etc.)	Structured Light	Kinect V1	Color, Depth	Eye Points	255 Sequences (76500 Frames)
Dexter 1	[216]	2013	Part Of Body (hand, Head, Etc.)	SCS, Structured Light, TOF	Kinect V1, Creative Gesture Camera, Stereo Camera	Color, Depth	-	7 Sequences
-	[217]	2013	Part Of Body (hand, Head, Etc.)	TOF	SoftKinetic DS 325	Color, Depth, Measurand ShapeHand	-	870 Images (30 Subjects)
MSRC-12 Kinect Gesture	[218]	2012	Part Of Body (hand, Head, Etc.)	Structured Light	Kinect V1	Color, Depth	-	594 Sequences (719359 Frames)
MSR Gesture3D	[205]	2012	Part Of Body (hand, Head, Etc.)	Structured Light	Kinect V1	Depth	-	336 Sequences
Florence 3D Faces	[219]	2011	Part Of Body (hand, Head, Etc.)	-	Synthetic	Color	-	53 People (N/A Frames/Seqs)

We found only four datasets available in this category, of which three of them contain endoscopic data and one contains 3D models of the iris. The most cited dataset in containing depth information in the medical field is:

Colonoscopy CG Dataset. This dataset is composed of endoscopic data of the colon. To the best of our knowledge, this is the most frequent type of data that contains depth maps in the Medical category, even if analyzing datasets with non-shared data. The authors generated a synthetic dataset using Unity graphic engine based on a human CT colonography scan. They extracted a surface mesh using manual segmentation and meshing [220]. Their work also proposed and tested an algorithm in real data, but this data is not available for the community thus not included in this paper.

Table 10: Datasets of “Medical” Category.

Dataset Name	Ref.	Year	Scene Type	Sensor Type	Sensor Name	Data Modalities	Extra Data	Images/Scenes
SCARED	[221]	2021	Endoscopy	SCS, Structured Light	Structured Light System (using P300 Neo Pico), Stereo Camera	Color, Depth	-	9 Sequences
Colonoscopy CG	[220]	2019	Endoscopy	-	Synthetic	Color, Depth	-	16016 Images
Endoscopic Video	[222]	2010	Endoscopy	SCS	Stereo Camera	Color	-	25 Scenes
-	[223]	2020	Iris Scan	-	Synthetic	Color, Depth	-	100 Irises (72k Images)

5. Discussion

The datasets presented in Section 4 compose a collection of different scenes, sensors, and activities. Despite this variety of datasets, we identified common tendencies in all areas and discussed them in this section.

Although synthetic data is becoming more present each time, the usage of real data is presented in the majority of the datasets. Comparing the 2016-2018 to the 2019-2021 trienniums, we found a 50% increase in the numbers of datasets containing synthetic data. Synthetic datasets are usually cheaper to produce than performing real data acquisition because extra annotations, e.g., semantic segmentation or object tracking, are automatically generated. On the other hand, complex scene annotations for real data are costly, especially in scenes such as driving and aerial.

Synthetic datasets were initially created using simulators [171; 170], but these simulators were distinct to real-world scenarios since the computational power of the machines was limited. Hence, it was not possible to generate consistent and realistic datasets for complex scenes. Recently, realistic simulators were created for driving scenes, such as CARLA [224], Nvidia Drive Sim², and indoor scenes, such as Habitat [225; 226]. Despite the usage of simulators, other datasets rely on game engines or general computer graphics engines to build their systems, such as SYNTHIA [99], Virtual KITTI [87], and Virtual KITTI 2 [88] that used Unity³ as graphic engine, and GTA-SfM [142] that uses scenes from the game GTAV.

The usage of synthetic data has been combined with real data to produce more complex scenes. These are applied especially for techniques that explore the generalization of their methods in non-expected scenes, i.e., using datasets not used in the training step [85; 16; 138].

These papers combine datasets containing different types of acquisition and scenes to produce generalizable models. Ranftl et al. [16] created multiple cross-dataset training strategies, and its combination of datasets with more images —called MIX5— contains data from DIML, MegaDepth, RedWeb, WSVD, and 3D Movies datasets. Ranftl et al. [227] expanded this combination, creating the MIX6 cross-dataset set containing about 1.4 million training images. Both works were evaluated using a mixture of testing datasets. The robustness of the models are also evaluated in a cross-dataset strategy for estimating depth from a monocular video [228], and instead of testing in multiple types of scenes, Ji et al. [229] combined distinct datasets of the same type of scene to improve the results for the indoor environment.

Recently, domain adaptation has been applied to improve the performance of the combination of datasets in the training step [230; 231; 232]. Atapour-Abarghouei and Breckon [231], for instance, combines one synthetic and one real dataset using domain adaptation to improve the result of training. They claim that directly using synthetic data may not improve the results for realistic data evaluation due to dataset bias. They adapt the domain of a synthetic dataset to a real

²<https://developer.nvidia.com/drive/drive-sim>

³<https://unity.com/>

dataset using Style Transfer and combine them to train their models. Zhao et al. [232] also performs domain adaptation, and they claim that due to the lack of paired synthetic and real images, the synthetic-to-realistic image translation adds distortions to the depth estimation. They overcome this difficulty by exploring a more complex training procedure involving synthetic-to-realistic and realistic-to-synthetic translations. In addition to using synthetic data, domain adaptation could also be applied to real-to-real translation [233; 234] since the dataset bias also affects distinct real datasets, especially by variations of scale and capture’s position of the scenes [235].

6. Conclusions

In this work, we presented a survey of publicly available image datasets that contain depth information. We categorized and summarized over 200 datasets based on the image scenes, sensors used to collect the depth information, and the different applications for which these datasets can be used. Almost half of the datasets we describe were proposed after the publication of the last survey [18]. The new datasets expand the scope of applications that depth datasets can be used for, such as medical applications. The new datasets also expand the quality and quantity of data for other areas.

We also presented different forms of acquiring depth information from a scene. We expect that this explanation could be used in conjunction with extra information of the datasets to allow researchers to choose the ones that best fulfill their needs. Researchers of zero-shot learning trying to increase generalization capabilities for their model could also benefit from our work since they may select distinct datasets in terms of sensor type, application, and scene type for training and evaluating their methods.

References

- [1] X. Luo, J.-B. Huang, R. Szeliski, K. Matzen, J. Kopf, Consistent Video Depth Estimation, *ACM Transactions on Graphics (ToG)* (2020) 71–1.
- [2] I. Lenz, H. Lee, A. Saxena, Deep Learning for Detecting Robotic Grasps, *The International Journal of Robotics Research* (2015) 705–724.
- [3] J. Xie, R. Girshick, A. Farhadi, Deep3D: Fully Automatic 2D-To-3D Video Conversion With Deep Convolutional Neural Networks, in: *European Conference on Computer Vision (ECCV)*, 2016, pp. 842–857.
- [4] D. Stoyanov, M. V. Scanzanella, P. Pratt, G.-Z. Yang, Real-Time Stereo Reconstruction In Robotically Assisted Minimally Invasive Surgery, in: *International Conference on Medical Image Computing and Computer-Assisted Intervention*, 2010, pp. 275–282.
- [5] J. Levinson, J. Askeland, J. Becker, J. Dolson, D. Held, S. Kammel, J. Z. Kolter, D. Langer, O. Pink, V. Pratt, M. Sokolsky, G. Stanek, D. Stavens, A. Teichman, M. Werling, S. Thrun, Towards Fully Autonomous Driving: Systems and Algorithms, in: *IEEE Intelligent Vehicles Symposium (IV)*, 2011, pp. 163–168.
- [6] S. M. H. Miangoleh, S. Dille, L. Mai, S. Paris, Y. Aksoy, Boosting Monocular Depth Estimation Models To High-Resolution Via Content-Adaptive Multi-Resolution Merging, in: *IEEE Conference on Computer Vision and Pattern Recognition (CVPR)*, 2021, pp. 9685–9694.

- [7] J. Uhrig, N. Schneider, L. Schneider, U. Franke, T. Brox, A. Geiger, Sparsity Invariant Cnns, in: International Conference on 3D Vision (3DV), 2017, pp. 11–20.
- [8] J. Tan, W. Lin, A. X. Chang, M. Savva, Mirror3D: Depth Refinement for Mirror Surfaces, in: IEEE Conference on Computer Vision and Pattern Recognition (CVPR), 2021, pp. 15990–15999.
- [9] J. Sturm, N. Engelhard, F. Endres, W. Burgard, D. Cremers, A Benchmark for The Evaluation Of RGB-D Slam Systems, in: IEEE/RISJ International Conference on Intelligent Robots and Systems, 2012, pp. 573–580.
- [10] A. Dai, A. X. Chang, M. Savva, M. Halber, T. Funkhouser, M. Nießner, Scannet: Richly-Annotated 3D Reconstructions Of Indoor Scenes, in: IEEE Conference on Computer Vision and Pattern Recognition (CVPR), 2017, pp. 2432–2443.
- [11] J. McCormac, A. Handa, S. Leutenegger, A. J. Davison, Scenenet RGB-D: Can 5M Synthetic Images Beat Generic Imagenet Pre-Training On Indoor Segmentation?, in: IEEE International Conference on Computer Vision (ICCV), 2017, pp. 2697–2706.
- [12] J. Zhang, W. Li, P. Wang, P. Ogunbona, S. Liu, C. Tang, A Large Scale RGB-D Dataset for Action Recognition, in: International Workshop on Understanding Human Activities through 3D Sensors, 2016, pp. 101–114.
- [13] Z. Li, N. Snavely, Megadepth: Learning Single-View Depth Prediction From Internet Photos, in: IEEE Conference on Computer Vision and Pattern Recognition (CVPR), 2018, pp. 2041–2050.
- [14] K. Xian, J. Zhang, O. Wang, L. Mai, Z. Lin, Z. Cao, Structure-Guided Ranking Loss for Single Image Depth Prediction, in: IEEE Conference on Computer Vision and Pattern Recognition (CVPR), 2020, pp. 611–620.
- [15] R. Ranftl, A. Bochkovskiy, V. Koltun, Vision Transformers for Dense Prediction, in: IEEE Conference on Computer Vision and Pattern Recognition (CVPR), 2021, pp. 12179–12188.
- [16] R. Ranftl, K. Lasinger, D. Hafner, K. Schindler, V. Koltun, Towards Robust Monocular Depth Estimation: Mixing Datasets for Zero-Shot Cross-Dataset Transfer, IEEE Transactions on Pattern Analysis and Machine Intelligence (TPAMI) (2020) 1–14.
- [17] M. Firman, RGBD Datasets: Past, Present and Future, in: IEEE Conference on Computer Vision and Pattern Recognition Workshops (CVPRW), 2016, pp. 19–31.
- [18] Z. Cai, J. Han, L. Liu, L. Shao, RGB-D Datasets Using Microsoft Kinect Or Similar Sensors: A Survey, Multimedia Tools and Applications (2017) 4313–4355.
- [19] R. B. Fisher, K. Konolige, Range Sensors, 2008, pp. 521–542.
- [20] J. Choi, Range Sensors: Ultrasonic Sensors, Kinect, and LiDAR, 2019, pp. 2521–2538.
- [21] J. Salvi, J. Pagès, J. Batlle, Pattern Codification Strategies In Structured Light Systems, Pattern Recognition (2004) 827–849.
- [22] M. O’Toole, S. Achar, S. G. Narasimhan, K. N. Kutulakos, Homogeneous Codes for Energy-Efficient Illumination and Imaging, ACM Transactions on Graphics (ToG) (2015) 1–13.

- [23] W. Kazmi, S. Foix, G. Alenya, Plant Leaf Imaging Using Time Of Flight Camera Under Sunlight, Shadow and Room Conditions, in: IEEE International Symposium on Robotic and Sensors Environments Proceedings, 2012, pp. 192–197.
- [24] B. Buttgen, P. Seitz, Robust Optical Time-Of-Flight Range Imaging Based On Smart Pixel Structures, IEEE Transactions on Circuits and Systems I: Regular Papers (2008) 1512–1525.
- [25] M. Jokela, M. Kuttila, P. Pyykönen, Testing and Validation Of Automotive Point-Cloud Sensors In Adverse Weather Conditions, Applied Sciences (2019) 2341.
- [26] A. G. Kashani, M. J. Olsen, C. E. Parrish, N. Wilson, A Review Of LIDAR Radiometric Processing: From Ad Hoc Intensity Correction To Rigorous Radiometric Calibration, Sensors (2015) 28099–28128.
- [27] J. Zbontar, Y. LeCun, Computing The Stereo Matching Cost With A Convolutional Neural Network, in: IEEE Conference on Computer Vision and Pattern Recognition (CVPR), 2015, pp. 1592–1599.
- [28] N. Silberman, D. Hoiem, P. Kohli, R. Fergus, Indoor Segmentation and Support Inference From RGBD Images, in: European Conference on Computer Vision (ECCV), 2012, pp. 746–760.
- [29] P. Ammirato, P. Poirson, E. Park, J. Kosecka, A. C. Berg, A Dataset for Developing and Benchmarking Active Vision, in: IEEE International Conference on Robotics and Automation (ICRA), 2017, pp. 1378–1385.
- [30] A. Geiger, P. Lenz, C. Stiller, R. Urtasun, Vision Meets Robotics: The KITTI Dataset, International Journal of Robotics Research (IJRR) (2013) 1231–1237.
- [31] K. Xian, C. Shen, Z. Cao, H. Lu, Y. Xiao, R. Li, Z. Luo, Monocular Relative Depth Perception With Web Stereo Data Supervision, in: IEEE Conference on Computer Vision and Pattern Recognition (CVPR), 2018, pp. 311–320.
- [32] F. Rowe, What Literature Review Is Not: Diversity, Boundaries and Recommendations, European Journal of Information Systems (2014) 241–255.
- [33] K. Yousif, A. Bab-Hadiashar, R. Hoseinnezhad, An Overview To Visual Odometry and Visual Slam: Applications To Mobile Robotics, Intelligent Industrial Systems (2015) 289–311.
- [34] T. Shen, Z. Luo, L. Zhou, R. Zhang, S. Zhu, T. Fang, L. Quan, Matchable Image Retrieval By Learning From Surface Reconstruction, in: The Asian Conference on Computer Vision (ACCV), 2018, pp. 415–431.
- [35] P. Wang, X. Huang, X. Cheng, D. Zhou, Q. Geng, R. Yang, The Apolloscape Open Dataset for Autonomous Driving and Its Application, IEEE transactions on pattern analysis and machine intelligence (2019) 2702–2719.
- [36] J. Jeong, Y. Cho, Y.-S. Shin, H. Roh, A. Kim, Complex Urban Dataset With Multi-Level Sensors From Highly Diverse Urban Environments, International Journal of Robotics Research (2019) 642–657.
- [37] W. Maddern, G. Pascoe, C. Linegar, P. Newman, 1 Year, 1000Km: The Oxford Robotcar Dataset, The International Journal of Robotics Research (IJRR) (2017) 3–15.

- [38] J.-L. Blanco-Claraco, F.-A. Moreno-Duenas, J. González-Jiménez, The Málaga Urban Dataset: High-Rate Stereo and LiDAR In A Realistic Urban Scenario, *The International Journal of Robotics Research* (2014) 207–214.
- [39] M. Schönbein, T. Strauß, A. Geiger, Calibrating and Centering Quasi-Central Catadioptric Cameras, in: *IEEE International Conference on Robotics and Automation (ICRA)*, 2014, pp. 4443–4450.
- [40] G. Pandey, J. R. McBride, R. M. Eustice, Ford Campus Vision and Lidar Data Set, *The International Journal of Robotics Research* (2011) 1543–1552.
- [41] A. Geiger, J. Ziegler, C. Stiller, Stereoscan: Dense 3D Reconstruction In Real-Time, in: *IEEE Intelligent Vehicles Symposium (IV)*, 2011, pp. 963–968.
- [42] Z. Zhang, H. Rebecq, C. Forster, D. Scaramuzza, Benefit Of Large Field-Of-View Cameras for Visual Odometry, in: *IEEE International Conference on Robotics and Automation (ICRA)*, 2016, pp. 801–808.
- [43] B. Zeisl, K. Koser, M. Pollefeys, Automatic Registration Of RGB-D Scans Via Salient Directions, in: *IEEE International Conference on Computer Vision (ICCV)*, 2013, pp. 2808–2815.
- [44] Y. Yao, Z. Luo, S. Li, J. Zhang, Y. Ren, L. Zhou, T. Fang, L. Quan, BlendedMVS: A Large-Scale Dataset for Generalized Multi-View Stereo Networks, *IEEE Conference on Computer Vision and Pattern Recognition (CVPR)* (2020) 1790–1799.
- [45] W. Chen, S. Qian, J. Deng, Learning Single-Image Depth From Videos Using Quality Assessment Networks, in: *IEEE Conference on Computer Vision and Pattern Recognition (CVPR)*, 2019, pp. 5604–5613.
- [46] C. Malleson, J. Guillemaut, A. Hilton, Hybrid Modeling Of Non-Rigid Scenes From RGBD Cameras, *IEEE Transactions on Circuits and Systems for Video Technology* (2019) 2391–2404.
- [47] K. Honauer, O. Johannsen, D. Kondermann, B. Goldluecke, A Dataset and Evaluation Methodology for Depth Estimation On 4D Light Fields, in: *The Asian Conference on Computer Vision (ACCV)*, 2016, pp. 19–34.
- [48] S. K. Ramakrishnan, A. Gokaslan, E. Wijmans, O. Maksymets, A. Clegg, J. Turner, E. Undersander, W. Galuba, A. Westbury, A. X. Chang, et al., Habitat-Matterport 3D Dataset (Hm3D): 1000 Large-Scale 3D Environments for Embodied AI, *arXiv preprint arXiv:2109.08238* (2021) 1–21.
- [49] C. X. Lu, M. R. U. Saputra, P. Zhao, Y. Almalioglu, P. P. B. de Gusmao, C. Chen, K. Sun, N. Trigoni, A. Markham, Milliego: Single-Chip Mmwave Radar Aided Egomotion Estimation Via Deep Sensor Fusion, in: *Proceedings of the 18th Conference on Embedded Networked Sensor Systems*, 2020, p. 109–122.
- [50] P. K. Lai, S. Xie, J. Lang, R. Laganière, Real-Time Panoramic Depth Maps From Omni-Directional Stereo Images for 6 Dof Videos In Virtual Reality, in: *IEEE Conference on Virtual Reality and 3D User Interfaces (VR)*, 2019, pp. 405–412.

- [51] N. Zioulis, A. Karakottas, D. Zarpalas, P. Daras, Omnidepth: Dense Depth Estimation for Indoors Spherical Panoramas, in: European Conference on Computer Vision (ECCV), 2018, pp. 448–465.
- [52] F.-E. Wang, H.-N. Hu, H.-T. Cheng, J.-T. Lin, S.-T. Yang, M.-L. Shih, H.-K. Chu, M. Sun, Self-supervised learning of depth and camera motion from 360 °videos, in: The Asian Conference on Computer Vision (ACCV), 2018, pp. 53–68.
- [53] O. Wasenmüller, M. Meyer, D. Stricker, Corbs: Comprehensive RGB-D Benchmark for Slam Using Kinect V2, in: IEEE Winter Conference on Applications of Computer Vision (WACV), 2016, pp. 1–7.
- [54] M. Burri, J. Nikolic, P. Gohl, T. Schneider, J. Rehder, S. Omari, M. W. Achtelik, R. Siegwart, The Euroc Micro Aerial Vehicle Datasets, The International Journal of Robotics Research (2016) 1157–1163.
- [55] S. Choi, Q.-Y. Zhou, V. Koltun, Robust Reconstruction Of Indoor Scenes, in: IEEE Conference on Computer Vision and Pattern Recognition (CVPR), 2015, pp. 5556–5565.
- [56] Y. Li, A. Dai, L. Guibas, M. Nießner, Database-Assisted Object Retrieval for Real-Time 3D Reconstruction, in: Computer Graphics Forum, 2015, pp. 435–446.
- [57] J. Martínez-Gómez, I. García-Varea, M. Cazorla, V. Morell, VidriLO: The Visual and Depth Robot Indoor Localization With Objects Information Dataset, The International Journal of Robotics Research (2015) 1681–1687.
- [58] A. Handa, T. Whelan, J. McDonald, A. J. Davison, A Benchmark for RGB-D Visual Odometry, 3D Reconstruction and Slam, in: IEEE International Conference on Robotics and Automation (ICRA), 2014, pp. 1524–1531.
- [59] D. Vautreydaz, A. Nègre, MobileRGBD, An Open Benchmark Corpus for Mobile RGB-D Related Algorithms, in: 13th International Conference on Control Automation Robotics & Vision (ICARCV), 2014, pp. 1668–1673.
- [60] K. Lai, L. Bo, D. Fox, Unsupervised Feature Learning for 3D Scene Labeling, in: IEEE International Conference on Robotics and Automation (ICRA), 2014, pp. 3050–3057.
- [61] O. Matusch, D. Panozzo, C. Mura, O. Sorkine-Hornung, R. Pajarola, Object Detection and Classification From Large-Scale Cluttered Indoor Scans, Computer Graphics Forum (2014) 11–21.
- [62] B. Glocker, S. Izadi, J. Shotton, A. Criminisi, Real-Time RGB-D Camera Relocalization, in: IEEE International Symposium on Mixed and Augmented Reality (ISMAR), 2013, pp. 173–179.
- [63] Q.-Y. Zhou, S. Miller, V. Koltun, Elastic Fragments for Dense Scene Reconstruction, in: IEEE International Conference on Computer Vision (ICCV), 2013, pp. 473–480.
- [64] F. Pomerleau, S. Magnenat, F. Colas, M. Liu, R. Siegwart, Tracking A Depth Camera: Parameter Exploration for Fast Icp, in: IEEE/RSJ International Conference on Intelligent Robots and Systems, 2011, pp. 3824–3829.

- [65] Q.-Y. Zhou, V. Koltun, Dense Scene Reconstruction With Points Of Interest, *ACM Transactions on Graphics (ToG)* (2013) 1–8.
- [66] S. Meister, S. Izadi, P. Kohli, M. Hämmerle, C. Rother, D. Kondermann, When Can We Use Kinectfusion for Ground Truth Acquisition, in: *Proc. Workshop on Color-Depth Camera Fusion in Robotics*, 2012, p. 3.
- [67] H. Ren, A. Raj, M. El-Khamy, J. Lee, Suw-Learn: Joint Supervised, Unsupervised, Weakly Supervised Deep Learning for Monocular Depth Estimation, in: *IEEE Conference on Computer Vision and Pattern Recognition Workshops (CVPRW)*, 2020, pp. 750–751.
- [68] Z. Li, T. Dekel, F. Cole, R. Tucker, N. Snavely, C. Liu, W. T. Freeman, Learning The Depths Of Moving People By Watching Frozen People, in: *IEEE Conference on Computer Vision and Pattern Recognition (CVPR)*, 2019, pp. 4516–4525.
- [69] A. Z. Zhu, D. Thakur, T. Özaskan, B. Pfrommer, V. Kumar, K. Daniilidis, The Multivehicle Stereo Event Camera Dataset: An Event Camera Dataset for 3D Perception, *IEEE Robotics and Automation Letters* (2018) 2032–2039.
- [70] T. Schöps, J. L. Schönberger, S. Galliani, T. Sattler, K. Schindler, M. Pollefeys, A. Geiger, A Multi-View Stereo Benchmark With High-Resolution Images and Multi-Camera Videos, in: *IEEE Conference on Computer Vision and Pattern Recognition (CVPR)*, 2017, pp. 2538–2547.
- [71] M. Li, Z. Zhou, Z. Wu, B. Shi, C. Diao, P. Tan, Multi-View Photometric Stereo: A Robust Solution and Benchmark Dataset for Spatially Varying Isotropic Materials, *IEEE Transactions on Image Processing* (2020) 4159–4173.
- [72] S. Choi, Q.-Y. Zhou, S. Miller, V. Koltun, A Large Dataset Of Object Scans, *arXiv preprint arXiv:1602.02481* (2016) 1–7.
- [73] M. Zollhöfer, A. Dai, M. Innmann, C. Wu, M. Stamminger, C. Theobalt, M. Nießner, Shading-Based Refinement On Volumetric Signed Distance Functions, *ACM Trans. Graph.* (2015) 1–14.
- [74] A. Singh, J. Sha, K. S. Narayan, T. Achim, P. Abbeel, Bigbird: A Large-Scale 3D Database Of Object Instances, in: *IEEE International Conference on Robotics and Automation (ICRA)*, 2014, pp. 509–516.
- [75] Q.-Y. Zhou, V. Koltun, Color Map Optimization for 3D Reconstruction With Consumer Depth Cameras, *ACM Transactions on Graphics (ToG)* (2014) 1–10.
- [76] R. Jensen, a. Dahl, G. Vogiatzis, E. Tola, H. Aanæs, Large Scale Multi-View Stereopsis Evaluation, in: *IEEE Conference on Computer Vision and Pattern Recognition (CVPR)*, 2014, pp. 406–413.
- [77] M. Ramezani, Y. Wang, M. Camurri, D. Wisth, M. Mattamala, M. Fallon, The Newer College Dataset: Handheld LiDAR, Inertial and Vision With Ground Truth, in: *IEEE/RSJ International Conference on Intelligent Robots and Systems (IROS)*, 2020, pp. 4353–4360.
- [78] Z. Li, N. Snavely, Megadepth: Learning Single-View Depth Prediction From Internet Photos, in: *IEEE Conference on Computer Vision and Pattern Recognition (CVPR)*, 2018, pp. 2041–2050.

- [79] F. Barrera Campo, F. Lumbreras Ruiz, A. D. Sappa, Multimodal Stereo Vision System: 3D Data Extraction and Algorithm Evaluation, *IEEE Journal of Selected Topics in Signal Processing* (2012) 437–446.
- [80] C.-C. Su, L. K. Cormack, A. C. Bovik, Color and Depth Priors In Natural Images, *IEEE Transactions on Image Processing* (2013) 2259–2274.
- [81] A. Saxena, M. Sun, A. Y. Ng, Make3D: Learning 3D Scene Structure From A Single Still Image, *IEEE Transactions on Pattern Analysis and Machine Intelligence* (2009) 824–840.
- [82] J. Schöning, G. Heidemann, Evaluation Of Multi-View 3D Reconstruction Software, in: *Computer Analysis of Images and Patterns*, 2015, pp. 450–461.
- [83] T. Beeler, F. Hahn, D. Bradley, B. Bickel, P. Beardsley, C. Gotsman, R. W. Sumner, M. Gross, High-Quality Passive Facial Performance Capture Using Anchor Frames, *ACM Trans. Graph.* (2011) 1–10.
- [84] A. Quattrini Li, A. Coskun, S. M. Doherty, S. Ghasemlou, A. S. Jagtap, M. Modasshir, S. Rahman, A. Singh, M. Xanthidis, J. M. O’Kane, I. Rekleitis, Experimental Comparison Of Open Source Vision-Based State Estimation Algorithms, in: *International Symposium on Experimental Robotics*, 2017, pp. 775–786.
- [85] B. Ummerhofer, H. Zhou, J. Uhrig, N. Mayer, E. Ilg, A. Dosovitskiy, T. Brox, Demon: Depth and Motion Network for Learning Monocular Stereo, in: *IEEE Conference on Computer Vision and Pattern Recognition (CVPR)*, 2017, pp. 5038–5047.
- [86] A. Geiger, P. Lenz, R. Urtasun, Are We Ready for Autonomous Driving? The KITTI Vision Benchmark Suite, in: *IEEE Conference on Computer Vision and Pattern Recognition (CVPR)*, 2012, pp. 3354–3361.
- [87] A. Gaidon, Q. Wang, Y. Cabon, E. Vig, Virtualworlds As Proxy for Multi-Object Tracking Analysis, in: *IEEE Conference on Computer Vision and Pattern Recognition (CVPR)*, 2016, pp. 4340–4349.
- [88] Y. Cabon, N. Murray, M. Humenberger, Virtual KITTI 2, *arXiv preprint arXiv:2001.10773* (2020) 1–11.
- [89] Y. Liao, J. Xie, A. Geiger, KITTI-360: A Novel Dataset and Benchmarks for Urban Scene Understanding In 2D and 3D, *arXiv preprint arXiv:2109.13410* (2021) 1–31.
- [90] S. Song, F. Yu, a. Zeng, A. X. Chang, M. Savva, T. Funkhouser, Semantic Scene Completion From A Single Depth Image, *IEEE Conference on Computer Vision and Pattern Recognition (CVPR)* (2017) 1746–1754.
- [91] L. Chen, F. Liu, Y. Zhao, W. Wang, X. Yuan, J. Zhu, Valid: A Comprehensive Virtual Aerial Image Dataset, in: *IEEE International Conference on Robotics and Automation (ICRA)*, 2020, pp. 2009–2016.
- [92] K. Foster, G. Christie, M. Brown, Urban Semantic 3D Dataset, 2020.

- [93] N. Haala, M. Cramer, K. Jacobsen, The German Camera Evaluation Project-Results From The Geometry Group, in: International Archives of the Photogrammetry, Remote Sensing and Spatial Information Sciences: Canadian Geomatics Conference and Symposium Of Commission I, ISPRS Convergence In Geomatics-Shaping Canada's Competitive Landscape, 2010, pp. 1–6.
- [94] F. Rottensteiner, G. Sohn, J. Jung, M. Gerke, C. Baillard, S. Benitez, U. Breitkopf, The Isprs Benchmark On Urban Object Classification and 3D Building Reconstruction, ISPRS Annals of the Photogrammetry, Remote Sensing and Spatial Information Sciences I-3 (2012) 293–298.
- [95] J.-L. Déziel, P. Merriaux, F. Tremblay, D. Lessard, D. Plourde, J. Stanguennec, P. Goulet, P. Olivier, Pixset : An Opportunity for 3D Computer Vision To Go Beyond Point Clouds With A Full-Waveform LiDAR Dataset, arXiv preprint arXiv:2102.12010 (2021) 1–8.
- [96] P. Sun, H. Kretzschmar, X. Dotiwalla, A. Chouard, V. Patnaik, P. Tsui, J. Guo, Y. Zhou, Y. Chai, B. Caine, et al., Scalability In Perception for Autonomous Driving: Waymo Open Dataset, in: IEEE Conference on Computer Vision and Pattern Recognition (CVPR), 2020, pp. 2446–2454.
- [97] M.-F. Chang, J. Lambert, P. Sangkloy, J. Singh, S. Bak, A. Hartnett, D. Wang, P. Carr, S. Lucey, D. Ramanan, J. Hays, Argoverse: 3D Tracking and Forecasting With Rich Maps, in: IEEE Conference on Computer Vision and Pattern Recognition (CVPR), 2019, pp. 8740–8749.
- [98] M. Cordts, M. Omran, S. Ramos, T. Rehfeld, M. Enzweiler, R. Benenson, U. Franke, S. Roth, B. Schiele, The Cityscapes Dataset for Semantic Urban Scene Understanding, in: IEEE Conference on Computer Vision and Pattern Recognition (CVPR), 2016, pp. 3213–3223.
- [99] G. Ros, L. Sellart, J. Materzynska, D. Vazquez, A. M. Lopez, The Synthia Dataset: A Large Collection Of Synthetic Images for Semantic Segmentation Of Urban Scenes, in: IEEE Conference on Computer Vision and Pattern Recognition (CVPR), 2016, pp. 3234–3243.
- [100] T. Scharwächter, M. Enzweiler, U. Franke, S. Roth, Stixmantics: A Medium-Level Model for Real-Time Semantic Scene Understanding, in: European Conference on Computer Vision (ECCV), 2014, pp. 533–548.
- [101] D. Pfeiffer, S. Gehrig, N. Schneider, Exploiting The Power Of Stereo Confidences, in: IEEE Conference on Computer Vision and Pattern Recognition (CVPR), 2013, pp. 297–304.
- [102] C. G. Keller, M. Enzweiler, D. M. Gavrila, A New Benchmark for Stereo-Based Pedestrian Detection, in: IEEE Intelligent Vehicles Symposium (IV), 2011, pp. 691–696.
- [103] M. Mancini, G. Costante, P. Valigi, T. A. Ciarfuglia, J-Mod 2: Joint Monocular Obstacle Detection and Depth Estimation, IEEE Robotics and Automation Letters (2018) 1490–1497.
- [104] W. Chen, S. Qian, D. Fan, N. Kojima, M. Hamilton, J. Deng, Oasis: A Large-Scale Dataset for Single Image 3D In The Wild, in: IEEE Conference on Computer Vision and Pattern Recognition (CVPR), 2020, pp. 679–688.

- [105] N. Mayer, E. Ilg, P. Häusser, P. Fischer, D. Cremers, A. Dosovitskiy, T. Brox, A Large Dataset To Train Convolutional Networks for Disparity, Optical Flow, and Scene Flow Estimation, in: IEEE Conference on Computer Vision and Pattern Recognition (CVPR), 2016, pp. 4040–4048.
- [106] H. Peng, B. Li, W. Xiong, W. Hu, R. Ji, RGBD Salient Object Detection: A Benchmark and Algorithms, in: European Conference on Computer Vision (ECCV), 2014, pp. 92–109.
- [107] N. Li, J. Ye, Y. Ji, H. Ling, J. Yu, Saliency Detection On Light Field, in: IEEE Conference on Computer Vision and Pattern Recognition (CVPR), 2014, pp. 2806–2813.
- [108] D. J. Butler, J. Wulff, G. B. Stanley, M. J. Black, A Naturalistic Open Source Movie for Optical Flow Evaluation, in: European Conference on Computer Vision (ECCV), 2012, pp. 611–625.
- [109] M. Ramamonjisoa, Y. Du, V. Lepetit, Predicting Sharp and Accurate Occlusion Boundaries In Monocular Depth Estimation Using Displacement Fields, in: IEEE Conference on Computer Vision and Pattern Recognition (CVPR), 2020, pp. 14636–14645.
- [110] A. Manglik, X. Weng, E. Ohn-Bar, K. M. Kitani, Forecasting Time-To-Collision From Monocular Video: Feasibility, Dataset, and Challenges, in: IEEE/RSJ International Conference on Intelligent Robots and Systems (IROS), 2019, pp. 8081–8088.
- [111] S. Song, S. P. Lichtenberg, J. Xiao, Sun RGB-D: A RGB-D Scene Understanding Benchmark Suite, in: IEEE Conference on Computer Vision and Pattern Recognition (CVPR), 2015, pp. 567–576.
- [112] A. Aldoma, T. Fäulhammer, M. Vincze, Automation Of "Ground Truth" Annotation for Multi-View RGB-D Object Instance Recognition Datasets, in: IEEE/RSJ International Conference on Intelligent Robots and Systems, 2014, pp. 5016–5023.
- [113] J. Mason, B. Marthi, R. Parr, Object Disappearance for Object Discovery, in: IEEE/RSJ International Conference on Intelligent Robots and Systems, 2012, pp. 2836–2843.
- [114] A. Janoch, S. Karayev, Y. Jia, J. T. Barron, M. Fritz, K. Saenko, T. Darrell, A Category-Level 3D Object Dataset: Putting The Kinect To Work, in: Consumer depth cameras for computer vision, 2013, pp. 141–165.
- [115] N. Silberman, R. Fergus, Indoor Scene Segmentation Using A Structured Light Sensor, in: IEEE International Conference on Computer Vision Workshops (ICCV Workshops), 2011, pp. 601–608.
- [116] S. Sajjan, M. Moore, M. Pan, G. Nagaraja, J. Lee, a. Zeng, S. Song, Clear Grasp: 3D Shape Estimation Of Transparent Objects for Manipulation, in: IEEE International Conference on Robotics and Automation (ICRA), 2020, pp. 3634–3642.
- [117] T. Hodaň, P. Haluza, Š. Obdržálek, J. Matas, M. Lourakis, X. Zabulis, T-Less: An RGB-D Dataset for 6D Pose Estimation Of Texture-Less Objects, IEEE Winter Conference on Applications of Computer Vision (WACV) (2017) 880–888.
- [118] D. Rotman, G. Gilboa, A Depth Restoration Occlusionless Temporal Dataset, in: Fourth International Conference on 3D Vision (3DV), 2016, pp. 176–184.

- [119] W. Susanto, M. Rohrbach, B. Schiele, 3D Object Detection With Multiple Kinects, in: European Conference on Computer Vision (ECCV), 2012, pp. 93–102.
- [120] M. Fonder, M. Van Droogenbroeck, Mid-Air: A Multi-Modal Dataset for Extremely Low Altitude Drone Flights, in: IEEE Conference on Computer Vision and Pattern Recognition Workshops (CVPRW), 2019, pp. 553–562.
- [121] S. Wu, L. Liebel, M. Körner, Derivation Of Geometrically and Semantically Annotated Uav Datasets At Large Scales From 3D City Models, in: International Conference on Pattern Recognition (ICPR), 2021, pp. 4712–4719.
- [122] D. Gehrig, M. Ruegg, M. Gehrig, J. Hidalgo-Carrio, D. Scaramuzza, Combining Events and Frames Using Recurrent Asynchronous Multimodal Networks for Monocular Depth Prediction, IEEE Robot and Automation Letters. (RA-L) (2021) 2822–2829.
- [123] V. Guizilini, R. Ambruş, S. Pillai, A. Raventos, A. Gaidon, 3D Packing for Self-Supervised Monocular Depth Estimation, in: IEEE Conference on Computer Vision and Pattern Recognition (CVPR), 2020, pp. 2482–2491.
- [124] J. Houston, G. Zuidhof, L. Bergamini, Y. Ye, L. Chen, A. Jain, S. Omari, V. Iglovikov, P. Ondruska, One Thousand and One Hours: Self-Driving Motion Prediction Dataset, arXiv preprint arXiv:2006.14480 (2020) 1–10.
- [125] H. Caesar, V. Bankiti, A. H. Lang, S. Vora, V. E. Liong, Q. Xu, A. Krishnan, Y. Pan, G. Baldan, O. Beijbom, Nuscenes: A Multimodal Dataset for Autonomous Driving, in: IEEE Conference on Computer Vision and Pattern Recognition (CVPR), 2020, pp. 11621–11631.
- [126] S. Yogamani, C. Hughes, J. Horgan, G. Sistu, P. Varley, D. O’Dea, M. Uricár, S. Milz, M. Simon, K. Amende, et al., Woodscape: A Multi-Task, Multi-Camera Fisheye Dataset for Autonomous Driving, in: IEEE Conference on Computer Vision and Pattern Recognition (CVPR), 2019, pp. 9308–9318.
- [127] M. Roberts, J. Ramapuram, A. Ranjan, A. Kumar, M. A. Bautista, N. Paczan, R. Webb, J. M. Susskind, Hypersim: A Photorealistic Synthetic Dataset for Holistic Indoor Scene Understanding, in: IEEE International Conference on Computer Vision (ICCV), 2021, pp. 10912–10922.
- [128] M. Deitke, W. Han, A. Herrasti, A. Kembhavi, E. Kolve, R. Mottaghi, J. Salvador, D. Schwenk, E. VanderBilt, M. Wallingford, et al., Robothor: An Open Simulation-To-Real Embodied AI Platform, in: IEEE Conference on Computer Vision and Pattern Recognition (CVPR), 2020, pp. 3164–3174.
- [129] J. Zheng, J. Zhang, J. Li, R. Tang, S. Gao, Z. Zhou, Structured3D: A Large Photo-Realistic Dataset for Structured 3D Modeling, in: European Conference on Computer Vision (ECCV), 2020, pp. 519–535.
- [130] J. Straub, T. Whelan, L. Ma, Y. Chen, E. Wijmans, S. Green, J. J. Engel, R. Mur-Artal, C. Ren, S. Verma, A. Clarkson, M. Yan, B. Budge, Y. Yan, X. Pan, J. Yon, Y. Zou, K. Leon, N. Carter, J. Briales, T. Gillingham, E. Mueggler, L. Pesqueira, M. Savva, D. Batra, H. M. Strasdat, R. D. Nardi, M. Goesele, S. Lovegrove, R. Newcombe, The REplica Dataset: A Digital Replica Of Indoor Spaces, arXiv preprint arXiv:1906.05797 (2019) 1–10.

- [131] F. Xia, A. R. Zamir, Z. He, A. Sax, J. Malik, S. Savarese, Gibson Env: Real-World Perception for Embodied Agents, in: IEEE Conference on Computer Vision and Pattern Recognition (CVPR), 2018, pp. 9068–9079.
- [132] W. Li, S. Saeedi, J. McCormac, R. Clark, D. Tzoumanikas, Q. Ye, Y. Huang, R. Tang, S. Leutenegger, Interiornet: Mega-Scale Multi-Sensor Photo-Realistic Indoor Scenes Dataset, in: British Machine Vision Conference (BMVC), 2018, pp. 1–13.
- [133] G. Garcia-Hernando, S. Yuan, S. Baek, T.-K. Kim, First-Person Hand Action Benchmark With RGB-D Videos and 3D Hand Pose Annotations, in: IEEE Conference on Computer Vision and Pattern Recognition (CVPR), 2018, pp. 409–419.
- [134] A. Chang, A. Dai, T. Funkhouser, M. Halber, M. Niessner, M. Savva, S. Song, a. Zeng, Y. Zhang, Matterport3D: Learning From RGB-D Data In Indoor Environments, in: International Conference on 3D Vision (3DV), 2017, pp. 667–676.
- [135] G. Georgakis, M. A. Reza, A. Mousavian, P.-H. Le, J. Košecká, Multiview RGB-D Dataset for Object Instance Detection, in: Fourth International Conference on 3D Vision (3DV), 2016, pp. 426–434.
- [136] I. Armeni, S. Sax, A. R. Zamir, S. Savarese, Joint 2D-3D-Semantic Data for Indoor Scene Understanding, arXiv preprint arXiv:1702.01105 (2017) 1–9.
- [137] J. Xiao, A. Owens, A. Torralba, Sun3D: A Database Of Big Spaces Reconstructed Using Sfm and Object Labels, in: IEEE International Conference on Computer Vision (ICCV), 2013, pp. 1625–1632.
- [138] A. Eftekhar, A. Sax, J. Malik, A. Zamir, Omnidata: A Scalable Pipeline for Making Multi-Task Mid-Level Vision Datasets From 3D Scans, in: IEEE International Conference on Computer Vision (ICCV), 2021, pp. 10786–10796.
- [139] K. Lai, L. Bo, X. Ren, D. Fox, A Large-Scale Hierarchical Multi-View RGB-D Object Dataset, in: IEEE International Conference on Robotics and Automation, 2011, pp. 1817–1824.
- [140] W. Wang, D. Zhu, X. Wang, Y. Hu, Y. Qiu, C. Wang, Y. Hu, A. Kapoor, S. Scherer, Tartanair: A Dataset To Push The Limits Of Visual Slam, in: IEEE/RSJ International Conference on Intelligent Robots and Systems (IROS), 2020, pp. 4909–4916.
- [141] F. Tombari, L. Di Stefano, S. Giardino, Online Learning for Automatic Segmentation Of 3D Data, in: IEEE/RSJ International Conference on Intelligent Robots and Systems, 2011, pp. 4857–4864.
- [142] K. Wang, S. Shen, Flow-Motion and Depth Network for Monocular Stereo and Beyond, IEEE Robotics and Automation Letters (2020) 3307–3314.
- [143] R. Lopez-Campos, J. Martinez-Carranza, Espada: Extended Synthetic and Photogrammetric Aerial-Image Dataset, IEEE Robotics and Automation Letters (2021) 1–1.
- [144] M. Gehrig, W. Aarents, D. Gehrig, D. Scaramuzza, DSEC: A Stereo Event Camera Dataset for Driving Scenarios, IEEE Robotics and Automation Letters (2021) 4947–4954.

- [145] M. L. Antequera, P. Gargallo, M. Hofinger, S. R. Bulò, Y. Kuang, P. Kotschieder, Mapillary Planet-Scale Depth Dataset, in: European Conference on Computer Vision (ECCV), 2020, pp. 589–604.
- [146] H. Schilling, M. Gutsche, A. Brock, D. Spath, C. Rother, K. Krispin, Mind The Gap-A Benchmark for Dense Depth Prediction Beyond Lidar, in: IEEE Conference on Computer Vision and Pattern Recognition Workshops (CVPRW), 2020, pp. 338–339.
- [147] G. Yang, X. Song, C. Huang, Z. Deng, J. Shi, B. Zhou, Drivingstereo: A Large-Scale Dataset for Stereo Matching In Autonomous Driving Scenarios, in: IEEE Conference on Computer Vision and Pattern Recognition (CVPR), 2019, pp. 899–908.
- [148] M. Mancini, G. Costante, P. Valigi, T. A. Ciarfuglia, J. Delmerico, D. Scaramuzza, Toward Domain Independence for Learning-Based Monocular Depth Estimation, *IEEE Robotics and Automation Letters* (2017) 1778–1785.
- [149] W. Yin, X. Wang, C. Shen, Y. Liu, Z. Tian, S. Xu, C. Sun, D. Renyin, Diversedepth: Affine-Invariant Depth Prediction Using Diverse Data, *arXiv preprint arXiv:2002.00569* (2020) 1–17.
- [150] K. Xian, J. Zhang, O. Wang, L. Mai, Z. Lin, Z. Cao, Structure-Guided Ranking Loss for Single Image Depth Prediction, in: IEEE Conference on Computer Vision and Pattern Recognition (CVPR), 2020, pp. 608–617.
- [151] Y. Hua, P. Kohli, P. Uplavikar, A. Ravi, S. Gunaseelan, J. Orozco, E. Li, Holopix50K: A Large-Scale In-The-Wild Stereo Image Dataset, in: CVPR Workshop on Computer Vision for Augmented and Virtual Reality, 2020, pp. 1–5.
- [152] R. Garg, N. Wadhwa, S. Ansari, J. T. Barron, Learning Single Camera Depth Estimation Using Dual-Pixels, in: IEEE International Conference on Computer Vision (ICCV), 2019, pp. 7628–7637.
- [153] Y. Gil, S. Elmaleh, H. Haim, E. Marom, R. Giryes, Monster: Awakening The Mono In Stereo, *arXiv preprint arXiv:1910.13708* (2019) 1–13.
- [154] C. Wang, S. Lucey, F. Perazzi, O. Wang, Web Stereo Video Supervision for Depth Prediction From Dynamic Scenes, in: International Conference on 3D Vision (3DV), 2019, pp. 348–357.
- [155] B. Keltjens, T. van Dijk, G. de Croon, Self-Supervised Monocular Depth Estimation of Untextured Indoor Rotated Scenes, *arXiv preprint arXiv:2106.12958* (2021) 1–13.
- [156] G. Albanis, N. Zioulis, P. Drakoulis, V. Gkitsas, V. Sterzentsenko, F. Alvarez, D. Zarpalas, P. Daras, Pano3D: A Holistic Benchmark and A Solid Baseline for 360Deg Depth Estimation, in: IEEE Conference on Computer Vision and Pattern Recognition (CVPR), 2021, pp. 3727–3737.
- [157] W. Yuan, R. Fan, M. Y. Wang, Q. Chen, Mfusetnet: Robust Depth Estimation With Learned Multiscopic Fusion, *IEEE Robotics and Automation Letters* (2020) 3113–3120.
- [158] Q. Wang, S. Zheng, Q. Yan, F. Deng, K. Zhao, X. Chu, Irs: A Large Naturalistic Indoor Robotics Stereo Dataset To Train Deep Models for Disparity and Surface Normal Estimation, *arXiv preprint arXiv:1912.09678* (2019) 1–12.

- [159] T. Koch, L. Liebel, F. Fraundorfer, M. Körner, Evaluation of CNN-Based Single-Image Depth Estimation Methods, in: European Conference on Computer Vision Workshops (ECCV-WS), 2019, pp. 331–348.
- [160] D. Scharstein, H. Hirschmüller, Y. Kitajima, G. Krathwohl, N. Nešić, X. Wang, P. Westling, High-Resolution Stereo Datasets With Subpixel-Accurate Ground Truth, in: German conference on pattern recognition, 2014, pp. 31–42.
- [161] D. Scharstein, C. Pal, Learning Conditional Random Fields for Stereo, in: IEEE Conference on Computer Vision and Pattern Recognition (CVPR), 2007, pp. 1–8.
- [162] D. Scharstein, R. Szeliski, High-Accuracy Stereo Depth Maps Using Structured Light, in: IEEE Conference on Computer Vision and Pattern Recognition (CVPR), 2003, pp. I–I.
- [163] I. Vasiljevic, N. Kolkin, S. Zhang, R. Luo, H. Wang, F. Z. Dai, andrea F. Daniele, M. Mostajabi, S. Basart, M. R. Walter, G. Shakhnarovich, DIODE: A DENSE INdoor and OUTdoor DEpth DATaset, arXiv preprint arXiv:1908.00463 (2019) 1–8.
- [164] J. Cho, D. Min, Y. Kim, K. Sohn, Deep Monocular Depth Estimation Leveraging A Large-Scale Outdoor Stereo Dataset, Expert Systems with Applications (2021) 114877.
- [165] J. Cui, L. Jin, H. Kuang, Q. Xu, S. Schwertfeger, Underwater Depth Estimation for Spherical Images, Journal of Robotics (2021) 6644986.
- [166] D. Berman, D. Levy, S. Avidan, T. Treibitz, Underwater Single Image Color Restoration Using Haze-Lines and A New Quantitative Dataset, IEEE Transactions on Pattern Analysis and Machine Intelligence (2021) 2822–2837.
- [167] J. Cho, D. Min, Y. Kim, K. Sohn, Deep Monocular Depth Estimation Leveraging A Large-Scale Outdoor Stereo Dataset, Expert Systems with Applications (2021) 114877.
- [168] H. Hirschmüller, D. Scharstein, Evaluation Of Cost Functions for Stereo Matching, IEEE Conference on Computer Vision and Pattern Recognition (CVPR) (2007) 1–8.
- [169] D. Scharstein, R. Szeliski, A Taxonomy and Evaluation Of Dense Two-Frame Stereo Correspondence Algorithms, International Journal of Computer Vision (2002) 7–42.
- [170] J.-P. Tarel, N. Hautiere, L. Caraffa, A. Cord, H. Halmaoui, D. Gruyer, Vision Enhancement In Homogeneous and Heterogeneous Fog, IEEE Intelligent Transportation Systems Magazine (2012) 6–20.
- [171] J.-P. Tarel, N. Hautiere, A. Cord, D. Gruyer, H. Halmaoui, Improved Visibility Of Road Scene Images Under Heterogeneous Fog, in: IEEE Intelligent Vehicles Symposium, 2010, pp. 478–485.
- [172] S. Niklaus, L. Mai, J. Yang, F. Liu, 3D Ken Burns Effect From A Single Image, ACM Transactions on Graphics (ToG) (2019) 1–15.
- [173] W. Chen, Z. Fu, D. Yang, J. Deng, Single-Image Depth Perception In The Wild, in: 30th International Conference on Neural Information Processing Systems, 2016, p. 730–738.

- [174] J. Tan, W. Lin, A. X. Chang, M. Savva, Mirror3D: Depth Refinement for Mirror Surfaces, in: IEEE Conference on Computer Vision and Pattern Recognition (CVPR), 2021, pp. 15985–15994.
- [175] S. Song, J. Xiao, Tracking Revisited Using RGBD Camera: Unified Benchmark and Baselines, in: IEEE International Conference on Computer Vision (ICCV), 2013, pp. 233–240.
- [176] J. Shin Yoon, K. Kim, O. Gallo, H. S. Park, J. Kautz, Novel View Synthesis Of Dynamic Scenes With Globally Coherent Depths From A Monocular Camera, in: IEEE Conference on Computer Vision and Pattern Recognition (CVPR), 2020, pp. 5335–5344.
- [177] P. P. Srinivasan, T. Wang, A. Sreelal, R. Ramamoorthi, R. Ng, Learning To Synthesize A 4D RGBD Light Field From A Single Image, in: IEEE International Conference on Computer Vision (ICCV), 2017, pp. 2243–2251.
- [178] J. Wang, Z. Liu, Y. Wu, J. Yuan, Mining Actionlet Ensemble for Action Recognition With Depth Cameras, in: IEEE Conference on Computer Vision and Pattern Recognition (CVPR), 2012, pp. 1290–1297.
- [179] J. Wang, X. Nie, Y. Xia, Y. Wu, S.-C. Zhu, Cross-View Action Modeling, Learning and Recognition, in: IEEE Conference on Computer Vision and Pattern Recognition (CVPR), 2014, pp. 2649–2656.
- [180] K. Yun, J. Honorio, D. Chattopadhyay, T. L. Berg, D. Samaras, Two-Person Interaction Detection Using Body-Pose Features and Multiple Instance Learning, in: IEEE Conference on Computer Vision and Pattern Recognition Workshops (CVPRW), 2012, pp. 28–35.
- [181] S. Hadfield, R. Bowden, Hollywood 3D: Recognizing Actions In 3D Natural Scenes, in: IEEE Conference on Computer Vision and Pattern Recognition (CVPR), 2013, pp. 3398–3405.
- [182] S. Tang, F. Tan, K. Cheng, Z. Li, S. Zhu, P. Tan, A Neural Network for Detailed Human Depth Estimation From A Single Image, in: IEEE International Conference on Computer Vision (ICCV), 2019, pp. 7749–7758.
- [183] C. Tang, W. Li, P. Wang, L. Wang, Online Human Action Recognition Based On Incremental Learning Of Weighted Covariance Descriptors, *Information Sciences* (2018) 219–237.
- [184] D. Liciotti, M. Paolanti, E. Frontoni, A. Mancini, P. Zingaretti, Person Re-Identification Dataset With RGB-D Camera In A Top-View Configuration, in: *Video Analytics. Face and Facial Expression Recognition and Audience Measurement*, 2017, pp. 1–11.
- [185] S. Gasparrini, E. Cippitelli, E. Gambi, S. Spinsante, J. Wåhslén, I. Orhan, T. Lindh, Proposal and Experimental Evaluation Of Fall Detection Solution Based On Wearable and Depth Data Fusion, in: *International conference on ICT innovations*, 2015, pp. 99–108.
- [186] S. Gasparrini, E. Cippitelli, E. Gambi, S. Spinsante, F. Florez-Revuelta, Performance Analysis Of Self-Organising Neural Networks Tracking Algorithms for Intake Monitoring Using Kinect, in: *IET International Conference on Technologies for Active and Assisted Living (TechAAL)*, 2015, pp. 1–6.

- [187] E. Cippitelli, S. Gasparri, E. Gambi, S. Spinsante, J. Wählény, I. Orhany, T. Lindhy, Time Synchronization and Data Fusion for RGB-Depth Cameras and Inertial Sensors In Aal Applications, in: IEEE International Conference on Communication Workshop (ICCW), 2015, pp. 265–270.
- [188] C. Chen, R. Jafari, N. Kehtarnavaz, Utd-Mhad: A Multimodal Dataset for Human Action Recognition Utilizing A Depth Camera and A Wearable Inertial Sensor, in: IEEE International conference on image processing (ICIP), 2015, pp. 168–172.
- [189] C. Ionescu, D. Papava, V. Olaru, C. Sminchisescu, Human3.6M: Large Scale Datasets and Predictive Methods for 3D Human Sensing In Natural Environments, IEEE Transactions on Pattern Analysis and Machine Intelligence (2014) 1325–1339.
- [190] S. Gasparri, E. Cippitelli, S. Spinsante, E. Gambi, A Depth-Based Fall Detection System Using A Kinect[®] Sensor, Sensors (2014) 2756–2775.
- [191] S. Escalera, J. González, X. Baró, M. Reyes, O. Lopes, I. Guyon, V. Athitsos, H. Escalante, Multi-Modal Gesture Recognition Challenge 2013: Dataset and Results, in: Proceedings of the 15th ACM on International conference on multimodal interaction, 2013, pp. 445–452.
- [192] F. Ofli, R. Chaudhry, G. Kurillo, R. Vidal, R. Bajcsy, Berkeley Mhad: A Comprehensive Multimodal Human Action Database, in: IEEE Workshop on Applications of Computer Vision (WACV), 2013, pp. 53–60.
- [193] I. Guyon, V. Athitsos, P. Jangyodsuk, H. J. Escalante, The Chalearn Gesture Dataset (Cgd 2011), Machine Vision and Applications (2014) 1929–1951.
- [194] R. Borràs, À. Lapedriza, L. Igual, Depth Information In Human Gait Analysis: An Experimental Study On Gender Recognition, in: International Conference Image Analysis and Recognition, 2012, pp. 98–105.
- [195] I. B. Barbosa, M. Cristani, A. Del Bue, L. Bazzani, V. Murino, Re-Identification With RGB-D Sensors, in: European Conference on Computer Vision (ECCV), 2012, pp. 433–442.
- [196] W. Li, Z. Zhang, Z. Liu, Action Recognition Based On A Bag Of 3D Points, in: IEEE Conference on Computer Vision and Pattern Recognition Workshops (CVPRW), 2010, pp. 9–14.
- [197] F. Yin, S. Zhou, Accurate Estimation Of Body Height From A Single Depth Image Via A Four-Stage Developing Network, in: IEEE Conference on Computer Vision and Pattern Recognition (CVPR), 2020, pp. 8267–8276.
- [198] T. Shu, M. S. Ryoo, S.-C. Zhu, Learning Social Affordance for Human-Robot Interaction, in: International Joint Conference on Artificial Intelligence (IJCAI), 2016, pp. 3454–3461.
- [199] H. Joo, T. Simon, X. Li, H. Liu, L. Tan, L. Gui, S. Banerjee, T. S. Godisart, B. Nabbe, I. Matthews, T. Kanade, S. Nobuhara, Y. Sheikh, Panoptic Studio: A Massively Multiview System for Social Interaction Capture, IEEE Transactions on Pattern Analysis and Machine Intelligence (2017) 190–204.
- [200] B. Kwolek, M. Kepski, Human Fall Detection On Embedded Platform Using Depth Maps and Wireless Accelerometer, Computer methods and programs in biomedicine (2014) 489–501.

- [201] L. Spinello, K. O. Arras, People Detection In RGB-D Data, in: IEEE/RSJ International Conference on Intelligent Robots and Systems, 2011, pp. 3838–3843.
- [202] Y. Tang, Y. Tian, J. Lu, J. Feng, J. Zhou, Action Recognition In RGB-D Egocentric Videos, in: IEEE International Conference on Image Processing (ICIP), 2017, pp. 3410–3414.
- [203] S. Stein, S. J. McKenna, Combining Embedded Accelerometers With Computer Vision for Recognizing Food Preparation Activities, in: ACM International Joint Conference on Pervasive and Ubiquitous Computing, 2013, pp. 729–738.
- [204] J. Tompson, M. Stein, Y. LeCun, K. Perlin, Real-Time Continuous Pose Recovery Of Human Hands Using Convolutional Networks, ACM Transactions on Graphics (ToG) (2014) 1–10.
- [205] J. Wang, Z. Liu, J. Chorowski, Z. Chen, Y. Wu, Robust 3D Action Recognition With Random Occupancy Patterns, in: European Conference on Computer Vision (ECCV), 2012, pp. 872–885.
- [206] J. Wang, F. Mueller, F. Bernard, S. Sorli, O. Sotnychenko, N. Qian, M. A. Otaduy, D. Casas, C. Theobalt, RGB2Hands: Real-Time Tracking Of 3D Hand Interactions From Monocular RGB Video, ACM Transactions on Graphics (ToG) (2020) 1–16.
- [207] Y. Hasson, G. Varol, D. Tzionas, I. Kalevatykh, M. J. Black, I. Laptev, C. Schmid, Learning Joint Reconstruction Of Hands and Manipulated Objects, in: IEEE Conference on Computer Vision and Pattern Recognition (CVPR), 2019, pp. 11807–11816.
- [208] S. Yuan, Q. Ye, B. Stenger, S. Jain, T.-K. Kim, BigHand2.2M Benchmark: Hand Pose Dataset and State Of The Art Analysis, in: IEEE Conference on Computer Vision and Pattern Recognition (CVPR), 2017, pp. 2605–2613.
- [209] G. Borghi, M. Venturelli, R. Vezzani, R. Cucchiara, Poseidon: Face-From-Depth for Driver Pose Estimation, in: IEEE Conference on Computer Vision and Pattern Recognition (CVPR), 2017, pp. 4661–4670.
- [210] C. Zimmermann, T. Brox, Learning to estimate 3d hand pose from single rgb images, in: IEEE Conference on Computer Vision and Pattern Recognition (CVPR), 2017, pp. 4903–4911.
- [211] J. Zhang, J. Jiao, M. Chen, L. Qu, X. Xu, Q. Yang, A Hand Pose Tracking Benchmark From Stereo Matching, in: IEEE International Conference on Image Processing (ICIP), 2017, pp. 982–986.
- [212] K. A. Funes Mora, F. Monay, J.-M. Odobez, Eyediap: A Database for The Development and Evaluation Of Gaze Estimation Algorithms From RGB and RGB-D Cameras, in: Proceedings of the Symposium on Eye Tracking Research and Applications, 2014, pp. 255–258.
- [213] R. Min, N. Kose, J.-L. Dugelay, Kinectfacedb: A Kinect Database for Face Recognition, Systems, Man, and Cybernetics: Systems, IEEE Transactions on (2014) 1534–1548.
- [214] E. E. Aksoy, M. Tamosiunaite, F. Wörgötter, Model-Free Incremental Learning Of The Semantics Of Manipulation Actions, Robotics and Autonomous Systems (2015) 118–133.

- [215] E. Nesli, S. Marcel, Spoofing In 2D Face Recognition With 3D Masks and Anti-Spoofing With Kinect, in: IEEE 6th International Conference on Biometrics: Theory, Applications and Systems (BTAS'13), 2013, pp. 1–8.
- [216] S. Sridhar, A. Oulasvirta, C. Theobalt, Interactive Markerless Articulated Hand Motion Tracking Using RGB and Depth Data, in: IEEE International Conference on Computer Vision (ICCV), 2013, pp. 2456–2463.
- [217] C. Xu, L. Cheng, Efficient Hand Pose Estimation From A Single Depth Image, in: IEEE International Conference on Computer Vision (ICCV), 2013, pp. 3456–3462.
- [218] S. Fothergill, H. Mentis, P. Kohli, S. Nowozin, Instructing People for Training Gestural Interactive Systems, in: Proceedings of the SIGCHI Conference on Human Factors in Computing Systems, 2012, p. 1737–1746.
- [219] A. D. Bagdanov, A. Del Bimbo, I. Masi, The Florence 2D/3D Hybrid Face Dataset, in: Joint ACM Workshop on Human Gesture and Behavior Understanding, 2011, p. 79–80.
- [220] A. Rau, P. E. Edwards, O. F. Ahmad, P. Riordan, M. Janatka, L. B. Lovat, D. Stoyanov, Implicit Domain Adaptation With Conditional Generative Adversarial Networks for Depth Prediction In Endoscopy, International Journal of Computer Assisted Radiology and Surgery (2019) 1–10.
- [221] M. Allan, J. Mcleod, C. Wang, J. C. Rosenthal, Z. Hu, N. Gard, P. Eisert, K. X. Fu, T. Zeffiro, W. Xia, et al., Stereo Correspondence and Reconstruction Of Endoscopic Data Challenge, arXiv preprint arXiv:2101.01133 (2021) 1–7.
- [222] P. Mountney, D. Stoyanov, G.-Z. Yang, Three-Dimensional Tissue Deformation Recovery and Tracking, IEEE Signal Processing Magazine (2010) 14–24.
- [223] D. P. Benalcazar, J. E. Zambrano, D. Bastias, C. A. Perez, K. W. Bowyer, A 3D Iris Scanner From A Single Image Using Convolutional Neural Networks, IEEE Access (2020) 98584–98599.
- [224] A. Dosovitskiy, G. Ros, F. Codevilla, A. Lopez, V. Koltun, Carla: An Open Urban Driving Simulator, in: Proceedings of the 1st Annual Conference on Robot Learning, 2017, pp. 1–16.
- [225] A. Szot, A. Clegg, E. Undersander, E. Wijmans, Y. Zhao, J. Turner, N. Maestre, M. Mukadam, D. Chaplot, O. Maksymets, A. Gokaslan, V. Vondrus, S. Dharur, F. Meier, W. Galuba, A. Chang, Z. Kira, V. Koltun, J. Malik, M. Savva, D. Batra, Habitat 2.0: Training Home Assistants To Rearrange Their Habitat, arXiv preprint arXiv:2106.14405 (2021) 1–16.
- [226] M. Savva, A. Kadian, O. Maksymets, Y. Zhao, E. Wijmans, B. Jain, J. Straub, J. Liu, V. Koltun, J. Malik, D. Parikh, D. Batra, Habitat: A Platform for Embodied AI Research, in: IEEE International Conference on Computer Vision (ICCV), 2019, pp. 9338–9346.
- [227] R. Ranftl, A. Bochkovskiy, V. Koltun, Vision transformers for dense prediction, in: IEEE Conference on Computer Vision and Pattern Recognition (CVPR), 2021, pp. 12179–12188.
- [228] J. Kopf, X. Rong, J.-B. Huang, Robust consistent video depth estimation, in: IEEE International Conference on Computer Vision (ICCV), 2021, pp. 1611–1621.

- [229] P. Ji, R. Li, B. Bhanu, Y. Xu, Monoindoor: Towards good practice of self-supervised monocular depth estimation for indoor environments, in: IEEE International Conference on Computer Vision (ICCV), 2021, pp. 12787–12796.
- [230] X. Guo, H. Li, S. Yi, J. Ren, X. Wang, Learning monocular depth by distilling cross-domain stereo networks, in: European Conference on Computer Vision (ECCV), 2018, pp. 484–500.
- [231] A. Atapour-Abarghouei, T. P. Breckon, Real-time monocular depth estimation using synthetic data with domain adaptation via image style transfer, in: IEEE Conference on Computer Vision and Pattern Recognition (CVPR), 2018, pp. 2800–2810.
- [232] S. Zhao, H. Fu, M. Gong, D. Tao, Geometry-aware symmetric domain adaptation for monocular depth estimation, in: IEEE Conference on Computer Vision and Pattern Recognition (CVPR), 2019, pp. 9788–9798.
- [233] A. Lopez-Rodriguez, K. Mikolajczyk, Desc: Domain adaptation for depth estimation via semantic consistency, arXiv preprint arXiv:2009.01579 (2020) 1–16.
- [234] J. Hornauer, L. Nalpantidis, V. Belagiannis, Visual domain adaptation for monocular depth estimation on resource-constrained hardware, in: IEEE Conference on Computer Vision and Pattern Recognition (CVPR), 2021, pp. 954–962.
- [235] A. Torralba, A. A. Efros, Unbiased look at dataset bias, in: IEEE Conference on Computer Vision and Pattern Recognition (CVPR), 2011, pp. 1521–1528.